JOURNAL OF GUIDANCE, CONTROL, AND DYNAMICS
Vol. 42, No. 11, November 2019

Adaptive Spacecraft Attitude Control Using Single-Gimbal Control Moment Gyroscopes Without Singularity Avoidance

Zhanzhan Zhao,* Gerardo Cruz,† and Dennis S. Bernstein‡
University of Michigan, Ann Arbor, Michigan 48109

DOI: 10.2514/1.G003926

This paper applies retrospective cost adaptive control (RCAC) to spacecraft attitude control with a rotation-matrix attitude parameterization using constant-speed single-gimbal control moment gyroscopes. Unlike control laws that use torque-steering laws to synthesize torque requests while avoiding gimbal singularities, the adaptive control law requests the rate of each gimbal. Because no torque request is provided, there is no need to invert the mapping from the gimbal rates to the control torque, and thus no attempt is made to avoid gimbal singularities. The RCAC implementation is based on a target model involving a single Markov parameter corresponding to the initial gimbal configuration. The parameters and weights for RCAC are based on nominal-model tuning, which uses no explicit knowledge of the nonlinear equations of motion. This paper investigates the robustness of RCAC to off-nominal conditions of commands, noise, and unknown bus inertia; and it examines the performance of RCAC in the case where an approximately singular gimbal configuration occurs during attitude command, following as well as the case of an initial gimbal-lock singularity. The performance of the adaptive controller in the presence of sensor/actuator misalignment is also investigated.

Nomenclature

A	=	attitude parameter matrix $\mathrm{diag}(a_1, a_2, a_3)$
a_1, a_2, a_3	=	attitude parameters
$B_{\mathrm{CMG}}, B_1, B_2$	=	control input matrices
c	=	center of mass of the spacecraft
c_i	=	center of mass of the ith wheel
e	=	rotation eigenaxis for the rotated bus inertia matrix $\vec{J}_{\mathrm{B,rot}}$
e_i	=	ith column of the 3×3 identity matrix I_3
e'	=	misalignment eigenaxis from $\mathrm{F_B}$ to $\mathrm{F_{B'}}$
$\mathrm{F_B}$	=	bus-fixed frame
$\mathrm{F_{B'}}$	=	sensor-fixed frame
$\mathrm{F_C}$	=	frame representing the attitude command for $\mathrm{F_B}$
$\mathrm{F_{G_i}}$	=	frame fixed to gimbal G_i
$\mathrm{F_I}$	=	inertial frame
$\mathrm{F_{W_i}}$	=	frame fixed to wheel W_i
G_i	=	ith gimbal
$G_{\mathrm{f}}(\mathbf{q})$	=	finite impulse response filter used by retrospective cost adaptive control
H	=	matrix that models the initial gimbal configuration used in G_{f}
I_3	=	3×3 identity matrix
J	=	inertia tensor $\vec{J}_{\mathrm{SC/c}}$ of the spacecraft relative to c resolved in $\mathrm{F_B}$
J_{B}	=	inertia tensor $\vec{J}_{\mathrm{B/c}}$ of the bus relative to c resolved in $\mathrm{F_B}$
$J_{\mathrm{B,rot}}$	=	rotated bus inertia matrix
J_i	=	inertia tensor $\vec{J}_{\mathrm{W}_i/\mathrm{c}_i}$ of W_i relative to c_i resolved in $\mathrm{F_{W_i}}$
$J_{i,\mathrm{c}}$	=	inertia tensor $\vec{J}_{\mathrm{W}_i/\mathrm{c}}$ of W_i relative to c resolved in $\mathrm{F_B}$
$\hat{J}_k(\hat{\Theta})$	=	retrospective cost function
k	=	discrete-time step
k_w	=	initial waiting period
l_z	=	dimension of z
l_u	=	dimension of u
l_Θ	=	dimension of Θ
m_i	=	mass of W_i
n	=	number of the gimbals
n_{c}	=	controller order
$\mathcal{O}_{\mathrm{B/G}_i}$	=	direction cosine matrix obtained by resolving $\vec{R}_{\mathrm{G}_i/\mathrm{B}}$ in $\mathrm{F_B}$
$\mathcal{O}_{\mathrm{B'/B}}$	=	direction cosine matrix obtained by resolving $\vec{R}_{\mathrm{B/B'}}$ in $\mathrm{F_{B'}}$
$\mathcal{O}_{\mathrm{B'/G}_i}$	=	direction cosine matrix obtained by resolving $\vec{R}_{\mathrm{G}_i/\mathrm{B'}}$ in $\mathrm{F_{B'}}$
$\mathcal{O}_i$	=	$\mathcal{O}_{\mathrm{B/G}_i}$
$\mathcal{O}_{i'}$	=	$\mathcal{O}_{\mathrm{B'/G}_i}$
$P_{i,k}$	=	controller coefficient matrix
$Q_{i,k}$	=	controller coefficient matrix
$\mathbf{q}$	=	forward shift operator
$\mathcal{R}_{\mathrm{B/I}}$	=	direction cosine matrix obtained by resolving $\vec{R}_{\mathrm{B/I}}$ in $\mathrm{F_B}$
$\mathcal{R}_{\mathrm{C/I}}$	=	direction cosine matrix obtained by resolving $\vec{R}_{\mathrm{C/I}}$ in $\mathrm{F_C}$
R_u	=	control weighting matrix $\eta_u I_{l_u}$
R_z	=	performance weighting matrix $\eta_z I_{l_z}$
R_Θ	=	regularization weighting matrix $\eta_\Theta I_{l_\Theta}$
$\tilde{\mathcal{R}}$	=	attitude-error rotation matrix between $\mathcal{R}_{\mathrm{B/I}}$ and $\mathcal{R}_{\mathrm{C/I}}$
$\vec{R}_{\mathrm{B/B'}}$	=	rotation tensor that rotates $\mathrm{F_{B'}}$ into $\mathrm{F_B}$
$\vec{R}_{\mathrm{B/I}}$	=	rotation tensor that rotates $\mathrm{F_I}$ into $\mathrm{F_B}$
$\vec{R}_{\mathrm{C/I}}$	=	rotation tensor that rotates $\mathrm{F_I}$ into $\mathrm{F_C}$
$\vec{R}_{\mathrm{G}_i/\mathrm{B}}$	=	rotation tensor that rotates $\mathrm{F_B}$ into $\mathrm{F_{G_i}}$
$\vec{R}_{\mathrm{G}_i/\mathrm{B'}}$	=	rotation tensor that rotates $\mathrm{F_{B'}}$ into $\mathrm{F_{G_i}}$
r_i	=	position of c_i relative to c resolved in $\mathrm{F_B}$
S	=	vector representation of the attitude error $\tilde{\mathcal{R}}$
s	=	scalar attitude-error metric
T_{s}	=	settling time to bring and maintain ϕ_{eig} within ϕ_∞
t	=	continuous-time variable
u	=	vector of gimbal rates
u_i	=	gimbal rate of G_i around $\hat{j}_{\mathrm{G}_i}$ relative to $\mathrm{F_B}$
W_i	=	ith wheel
z	=	performance variable
$\hat{z}_k$	=	retrospective performance variable

Received 22 June 2018; revision received 8 June 2019; accepted for publication 1 July 2019; published online 19 August 2019.

*Graduate Student, Department of Aerospace Engineering; zhanzhao@umich.edu.

†Staff Member, NASA Goddard Space Flight Center; gerardo.e.cruz-ortiz@nasa.gov.

‡Professor, Department of Aerospace Engineering; dsbaero@umich.edu.

α_i = moment of inertia of W_i around the spin axis $\hat{i}_{W_i}$
β = pyramidal face angle
β_i = moment of inertia of W_i around $\hat{j}_{W_i}$ and $\hat{k}_{W_i}$
Θ_k = controller coefficient vector
$\hat{\Theta}$ = retrospectively optimized controller coefficient vector
θ = rotation eigenangle for the rotated bus inertia matrix $J_{B,rot}$
θ_i = rotation angle of G_i
θ' = misalignment eigenangle from F_B to $F_{B'}$.
ν_i = spin rate of the frame F_{W_i} relative to F_{G_i} around $\hat{i}_{W_i}$
ξ_C = commanded eigenaxis resolved in F_I
τ_{CMG} = torque applied to the spacecraft by the control moment gyroscopes
τ_{dist} = torque applied to the spacecraft by the disturbances
τ_{G_i} = torque applied to the spacecraft by G_i
Φ_k = regressor matrix
ϕ_C = commanded eigenangle
ϕ_{eig} = rotation angle around the eigenaxis that rotates $\mathcal{R}_{B/I}(t)$ to $R_C(t)$
ϕ_∞ = bound on ϕ_{eig}
ω_B = angular velocity of F_B relative to F_I resolved in F_B
ω_C = angular velocity of F_C relative to F_I resolved in F_C
$\tilde{\omega}_B$ = angular velocity of F_B relative to F_C resolved in F_B
$\vec{\omega}_{B/I}$ = angular velocity of F_B relative to F_I
$\vec{\omega}_{C/I}$ = angular velocity of F_C relative to F_I

I. Introduction

A CONTROL moment gyroscope (CMG) consists of a spinning wheel mounted on one or two gimbals; the wheel may spin at either a constant or variable rate. The gimbal or gimbals rotate the wheel's spin axis relative to the spacecraft bus, thereby applying a reaction torque to the spacecraft. The high torque levels and accuracy provided by CMGs make them well suited for attitude control of large space stations, orbiting telescopes, and agile spacecraft [1–3].

CMGs are typically operated using torque-steering laws [2–6]. In Fig. 1,[§] the controller requests the torque τ_{req}, and the torque-steering law synthesizes the requested gimbal-rate control input u, resulting in the actuation torque τ_{CMG} applied to the spacecraft. When the control input matrix B_{CMG} becomes rank deficient, the torque τ_{CMG} along one direction cannot be generated, and thus all possible torque vectors are coplanar [4], which indicates a singular gimbal configuration. In Ref. [7], geometric methods are used to determine the CMG singular surfaces. If a CMG singularity can be reconfigured by null motion ($B_{CMG}(t)u(t) = 0$) into a nonsingular gimbal configuration, it is called hyperbolic or passable; otherwise, it is called elliptic or impassable [8].

Singularities are inherent in every array of constant-speed CMGs [5]. At the expense of greater hardware complexity, gimbal singularities do not arise with variable-speed CMGs [9,10]. Alternatively, Refs. [11,12] considered CMGs under rotor offset to avoid singularities. Singularities can be mitigated using singularity-avoidance torque-steering laws [13–23]. In particular, rapid escape from impassable internal singularities was discussed in Refs. [18,19,24].

Torque-steering laws based on adaptive control algorithms have been applied to both constant-speed and variable-speed CMGs. In particular, adaptive control of constant-speed single-gimbal CMGs was considered in Refs. [25–27]; adaptive control of double-gimbal CMGs was considered in Ref. [28]; and adaptive control of variable-speed CMGs was considered in Refs. [29,30].

[§]Note that e_{att} = attitude error and r_{att} = attitude command in Figs. 1 and 2 only.

In contrast to CMG-driven attitude control laws based on torque-steering laws, the present paper focuses on direct gimbal-rate-requested adaptive control of single-gimbal constant-speed CMGs without a torque-steering law. In Fig. 2, the controller directly requests the gimbal rates u without a torque-steering law, and thus without specifying a requested torque. The gimbal motors implement the requested gimbal rates u that, as a result of the CMG dynamics, produce the actuation torque τ_{CMG} applied to the spacecraft. Because no torque request is specified, there is no need to invert the mapping from the gimbal rates to the control torque, and thus no attempt is made to avoid gimbal singularities. The direct gimbal-rate approach was used in Refs. [31–33]. In particular, the approach of Ref. [31] was confined to open-loop control, Ref. [32] linearized the nonlinear system and applies an optimal control law, and Ref. [33] applied sliding mode control.

Nevertheless, approximate gimbal singularities can occur using the direct gimbal-rate approach. In these cases, the impact of singularities encountered during a maneuver is limited due to the fact that the control input matrix B_{CMG} is time dependent, and thus rank-deficient conditions tend to hold at only isolated points. This property thus facilitates a simplified approach to the use of constant-speed CMGs for spacecraft attitude control.

The adaptive control law adopted in the present paper is retrospective cost adaptive control (RCAC). RCAC was developed for linear systems in Refs. [34–36]. As shown in the present paper, RCAC requires extremely limited modeling information for a spacecraft with CMG actuation, namely, geometric information concerning the initial gimbal configuration. The ability of RCAC to control the spacecraft with limited modeling information is demonstrated by tuning RCAC in numerical simulations based on a nominal model and by subsequently evaluating its performance using a perturbed model. In this approach, the spacecraft equations of motion are used only for numerical simulation; no explicit knowledge of these equations is used by RCAC. Closed-loop stability for linear systems using RCAC was addressed in Ref. [35]. Proof of closed-loop stability for nonlinear systems in general and CMG control of spacecraft is an open problem.

A pyramidal CMG arrangement consisting of four CMGs is considered in this paper. The RCAC law is based on a rotation-matrix attitude parameterization, which avoids singularities arising with Euler angles and Rodrigues parameters as well as the double covering arising from quaternions. These issues and their ramifications were discussed in Refs. [37,38].

The specific contributions of this paper are as follows:

1) In contrast with torque-steering laws, a gimbal-rate controller is shown to achieve approximate singularity passthrough and escape from a singularity.

2) The adaptive controller uses no explicit knowledge of the spacecraft equations of motion, including the bus inertia and nonlinearities.

3) A robustness study demonstrates the performance of the adaptive controller over a wide range of unknown inertia matrices, and in the presence of sensor/actuator misalignment. These results extend preliminary results given in Refs. [39,40] and complement the application of RCAC to spacecraft with reaction wheels, magnetic torquers, and an appendage in Refs. [41–43].

The contents of the paper are as follows. Section II enumerates assumptions for a spacecraft actuated by a collection of constant-speed single-axis CMGs, and it summarizes the equations of motion. Section III defines the performance variable for the attitude control problem. Section IV briefly reviews RCAC. Section V describes the pyramidal arrangement of four CMGs and constructs the target model needed by RCAC for an initial gimbal configuration. Section VI investigates the performance of RCAC for a spacecraft controlled by CMGs in the pyramidal arrangement with sensor noise, off-nominal commands, an unknown bus inertia matrix, an approximate singularity passthrough, escape from an initially singular gimbal configuration, and sensor/actuator misalignment. Finally, the Appendix provides a derivation of the equations of motion for the spacecraft controlled by CMGs. This derivation shows explicitly how each assumption is used to arrive at the equations of motion used for nominal-model tuning and perturbed-model testing.

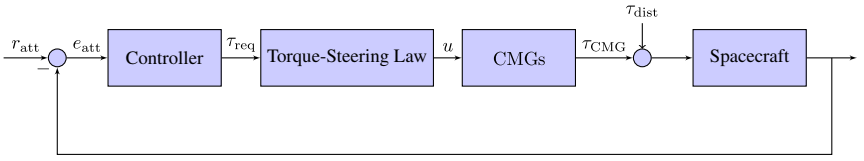

Fig. 1 The controller requests the torque τ_{req}, and the torque-steering law requests the gimbal rates u.

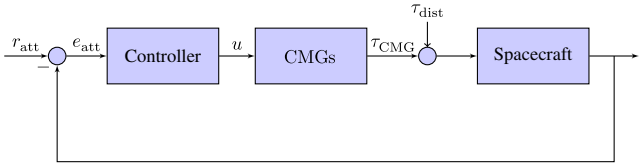

Fig. 2 The controller directly requests the gimbal rates u without a torque-steering law.

II. Spacecraft Attitude Dynamics with Direct Gimbal-Rate Request

The dynamics of a spacecraft SC consisting of a bus B and n single-gimbal constant-speed CMGs in an arbitrary arrangement are considered. For $i = 1, \ldots, n$, CMG_i is composed of wheel W_i mounted on gimbal G_i as shown in Fig. 3. Vectors denoted by $\vec{r}$ and second-order tensors denoted by $\vec{R}$ are component free.¶ Differentiation of component-free vectors and tensors is performed with respect to a frame; differentiation of resolved vectors and tensors does not require a frame.

A. Kinematics and Frames

Let F_I be an inertial frame, and let F_B be a bus frame defined by the pyramidal CMG arrangement as discussed in Sec. V. The rotational attitude kinematics of the bus are described by Poisson's equation

$$\overset{\text{B}\bullet}{\vec{R}}_{\text{B/I}} = \vec{R}_{\text{B/I}}\vec{\omega}^{\times}_{\text{B/I}} \tag{1}$$

where B• denotes the frame derivative with respect to F_B, $\vec{R}_{\text{B/I}}$ is the rotation tensor that rotates F_I into F_B (see footnote ¶), $\vec{\omega}_{\text{B/I}}$ is the angular velocity of F_B relative to F_I, and the superscript "×" denotes the skew-symmetric cross-product matrix. For all $i = 1, \ldots, n$, the frame F_{G_i} is fixed to G_i, and the frame F_{W_i} is fixed to W_i.

Resolving the second-order tensor $\vec{R}_{\text{B/I}}$ yields the rotation matrix

$$\mathcal{R}_{\text{B/I}} \triangleq \vec{R}_{\text{B/I}}\Big|_{\text{B}} = \vec{R}_{\text{B/I}}\Big|_{\text{I}} \tag{2}$$

which is a 3×3 direction cosine matrix. The second equality is due to the fact that the rotation tensor represents a rotation about an eigenaxis that is fixed in both frames. The orientation matrix $\mathcal{O}_{\text{B/I}}$ is defined by

$$\mathcal{O}_{\text{B/I}} = \mathcal{R}^{\text{T}}_{\text{B/I}} = \mathcal{R}_{\text{I/B}} \tag{3}$$

which is also a 3×3 direction cosine matrix. If $\vec{x}$ is a coordinate-free vector, then

$$\vec{x}|_{\text{B}} = \mathcal{O}_{\text{B/I}}\vec{x}|_{\text{I}} \tag{4}$$

and, if $\vec{J}$ is a second-order tensor, then

$$\vec{J}|_{\text{B}} = \mathcal{O}_{\text{B/I}}\vec{J}|_{\text{I}}\mathcal{O}_{\text{I/B}} \tag{5}$$

The following assumptions are made.

¶Kovecses, J., "Dynamics of Mechanical Systems Part 1: Concepts, Geometry and Kinematic Considerations," 2017, https://hal.archives-ouvertes.fr/hal-01534010 [retrieved 01 June 2019].

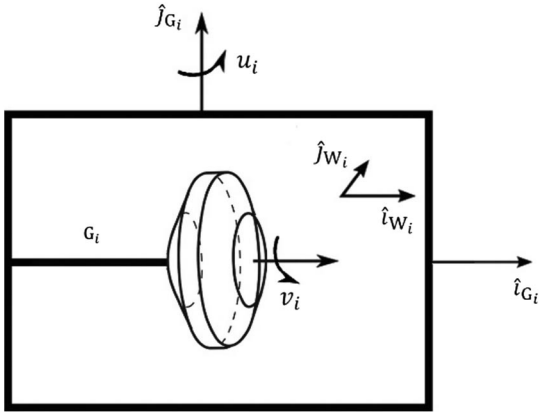

Fig. 3 Notation and conventions for CMG_i.

Assumption 1: The bus and wheels are rigid bodies.

Assumption 2: The gimbals are massless.

Assumption 3: For all $i = 1, \ldots, n$, the center of mass c_i of W_i is fixed in the bus.

Assumption 4: For all $i = 1, \ldots, n$, the direction of the axis $\hat{\imath}_{\text{W}_i}$ is fixed in F_{G_i}. In particular, $\hat{\imath}_{\text{W}_i} = \hat{\imath}_{\text{G}_i}$.

Assumption 5: For all $i = 1, \ldots, n$, the wheel W_i is inertially symmetric around $\hat{\imath}_{\text{W}_i}$.

Assumption 6: For all $i = 1, \ldots, n$, the frame F_{W_i} spins around $\hat{\imath}_{\text{W}_i}$ at the constant rate $\nu_i > 0$ relative to F_{G_i}.

Assumption 7: For all $i = 1, \ldots, n$, gimbal G_i is actuated by requesting its rate u_i around $\hat{\jmath}_{\text{G}_i}$ relative to F_B.

Figure 3 and Assumptions 4 and 5 imply that the inertia matrix of W_i relative to c_i resolved in both F_{G_i} and F_{W_i} is given by

$$J_i \triangleq \vec{J}_{\text{W}_i/\text{c}_i}|_{G_i} = \vec{J}_{\text{W}_i/\text{c}_i}|_{\text{W}_i} = \begin{bmatrix} \alpha_i & 0 & 0 \\ 0 & \beta_i & 0 \\ 0 & 0 & \beta_i \end{bmatrix} \tag{6}$$

where α_i is the moment of inertia of W_i around the spin axis $\hat{\imath}_{\text{W}_i} = \hat{\imath}_{\text{G}_i}$, and β_i is the moment of inertia around the remaining axes of F_{W_i} and F_{G_i}. Therefore,

$$\vec{J}_{\text{W}_i/\text{c}_i}|_{\text{B}} = \mathcal{O}_i\vec{J}_{\text{W}_i/\text{c}_i}|_{\text{G}_i}\mathcal{O}_i^{\text{T}} = \mathcal{O}_i J_i \mathcal{O}_i^{\text{T}} \tag{7}$$

and the 3×3 orientation matrix $\mathcal{O}_i$ is defined by

$$\mathcal{O}_i \triangleq \mathcal{O}_{\text{B/G}_i} = \vec{R}_{\text{G}_i/\text{B}}|_{\text{G}_i} = \vec{R}_{\text{G}_i/\text{B}}|_{\text{B}} \tag{8}$$

where $\vec{R}_{\text{G}_i/\text{B}}$ is the rotation tensor that rotates F_B into F_{G_i}. For a coordinate-free vector $\vec{x}$, $\vec{x}|_{\text{B}} = \mathcal{O}_i\vec{x}|_{\text{G}_i}$.

Next, define

$$J_{i,\text{c}} \triangleq \vec{J}_{\text{W}_i/\text{c}}|_{\text{B}} = \mathcal{O}_i J_i \mathcal{O}_i^{\text{T}} - m_i r_i^{\times 2}, \qquad r_i \triangleq \vec{r}_{\text{c}_i/\text{c}}|_{\text{B}} \tag{9}$$

where m_i is the mass of W_i. Note that r_i is the position of c_i relative to c resolved in F_B. Define the bus inertia matrix

$$J_{\text{B}} \triangleq \vec{J}_{\text{B/c}}|_{\text{B}}$$

Then, the inertia tensor of the spacecraft relative to its center of mass resolved in F_B is given by

$$J \triangleq \overrightarrow{J}_{\mathrm{SC/c}}|_{\mathrm{B}} = \overrightarrow{J}_{\mathrm{B/c}}|_{\mathrm{B}} + \sum_{i=1}^{n} \overrightarrow{J}_{\mathrm{W}_i/\mathrm{c}}|_{\mathrm{B}} = J_{\mathrm{B}} + \sum_{i=1}^{n} J_{i,\mathrm{c}} \quad (10)$$

B. Dynamics

In equation (4.81) of Ref. [4], setting the inertial derivative of the spacecraft angular momentum

$$\frac{{}^{N}\mathrm{d}\vec{H}}{\mathrm{d}t}$$

to be τ_{CMG} and setting the wheel angular accelerations to be zero yield

$$J\dot{\omega}_{\mathrm{B}} + \omega_{\mathrm{B}} \times \left(J\omega_{\mathrm{B}} + \sum_{i=1}^{n} \alpha_i \nu_i \mathcal{O}_i e_1 \right) = \tau_{\mathrm{CMG}} + \tau_{\mathrm{dist}} \quad (11)$$

where

$$\omega_{\mathrm{B}} \triangleq \vec{\omega}_{\mathrm{B/I}}|_{\mathrm{B}}$$

Note that τ_{dist} is the torque disturbance applied to the spacecraft, and the torque τ_{CMG} applied to the spacecraft by the CMGs is given by

$$\tau_{\mathrm{CMG}} \triangleq B_{\mathrm{CMG}} u + B_1 \dot{u} \quad (12)$$

$$B_{\mathrm{CMG}} \triangleq \omega_{\mathrm{B}}^{\times} B_1 - B_2 \in \mathbb{R}^{3\times n} \quad (13)$$

where the ith column of $B_1 \in \mathbb{R}^{3\times n}$ is given by

$$B_{1i} = -\beta_i \mathcal{O}_i e_2 \in \mathbb{R}^3 \quad (14)$$

and the ith column of $B_2 \in \mathbb{R}^{3\times n}$ is given by

$$B_{2i} = \mathcal{O}_i (e_2^{\times} J_i - J_i e_2^{\times}) \mathcal{O}_i^{\mathrm{T}} \omega_{\mathrm{B}} - \alpha_i \nu_i \mathcal{O}_i e_3 \in \mathbb{R}^3 \quad (15)$$

where e_i denotes the ith column of the 3×3 identity matrix I_3. As in Ref. [4] (p. 80), the term $B_1 \dot{u}$ is not considered in the subsequent development.

In Ref. [44], the equations of motion for a spacecraft controlled by constant-speed single-gimbal CMGs are derived where, in the notation of Ref. [44], $B_1 \dot{u}$ in Eq. (12) is expressed as $B\underline{\ddot{\sigma}}$ and $B_{\mathrm{CMG}} u$ is expressed as $(D_1 + D_2 + D_3)\underline{\dot{\sigma}}$. Various torque-steering laws involving $B\underline{\ddot{\sigma}}$, D_2, and D_3 were considered in Ref. [44]. In equation (4.81) in Ref. [4], the term

$$\sum_{i=1}^{n} \boldsymbol{J}_{g,i} \ddot{\delta}_i \hat{\mathbf{g}}_i$$

is equivalent to $B_1 \dot{u}$ in Eq. (12). Related developments appeared in Refs. [29,45].

III. Performance Variable for the Attitude Control Problem

A. Commanded Attitude and Attitude Error

Let $\mathrm{F_C}$ be a frame that represents the commanded attitude for $\mathrm{F_B}$. The control objective is to have the spacecraft attitude

$$\mathcal{R}_{\mathrm{B}} \triangleq \overrightarrow{R}_{\mathrm{B/I}}|_{\mathrm{B}}$$

follow the commanded attitude maneuver given by

$$\dot{\mathcal{R}}_{\mathrm{C/I}} = \frac{\mathrm{d}}{\mathrm{d}t}(\overrightarrow{R}_{\mathrm{C/I}}|_{\mathrm{C}}) = \overrightarrow{\dot{R}}^{\mathrm{C}\bullet}_{\mathrm{C/I}}|_{\mathrm{C}} = \overrightarrow{R}_{\mathrm{C/I}}|_{\mathrm{C}} \vec{\omega}_{\mathrm{C/I}}|_{\mathrm{C}}^{\times} = \mathcal{R}_{\mathrm{C/I}} \omega_{\mathrm{C}}^{\times} \quad (16)$$

where $\overrightarrow{R}_{\mathrm{C/I}}$ is the rotation tensor that rotates $\mathrm{F_I}$ into $\mathrm{F_C}$, $\vec{\omega}_{\mathrm{C/I}}$ is the angular velocity of $\mathrm{F_C}$ relative to $\mathrm{F_I}$, C• indicates the frame derivative with respect to $\mathrm{F_C}$, and

$$\mathcal{R}_{\mathrm{C/I}} \triangleq \overrightarrow{R}_{\mathrm{C/I}}|_{\mathrm{C}} = \overrightarrow{R}_{\mathrm{C/I}}|_{\mathrm{I}}, \qquad \omega_{\mathrm{C}} \triangleq \vec{\omega}_{\mathrm{C/I}}|_{\mathrm{C}} \quad (17)$$

The error between $\mathcal{R}_{\mathrm{B/I}}$ and $\mathcal{R}_{\mathrm{C/I}}$ is given in terms of the attitude-error rotation matrix

$$\begin{aligned}\tilde{\mathcal{R}} &\triangleq \overrightarrow{R}_{\mathrm{B/C}}|_{\mathrm{B}} = \overrightarrow{R}_{\mathrm{B/I}}|_{\mathrm{B}} \overrightarrow{R}_{\mathrm{I/C}}|_{\mathrm{B}} = \mathcal{R}_{\mathrm{B/I}} \overrightarrow{R}_{\mathrm{B/I}}|_{\mathrm{B}}^{\mathrm{T}} \overrightarrow{R}_{\mathrm{C/I}}|_{\mathrm{I}}^{\mathrm{T}} \overrightarrow{R}_{\mathrm{B/I}}|_{\mathrm{B}} \\ &= \mathcal{R}_{\mathrm{C/I}}^{\mathrm{T}} \mathcal{R}_{\mathrm{B/I}}\end{aligned} \quad (18)$$

which satisfies

$$\dot{\tilde{\mathcal{R}}} = \overrightarrow{\dot{R}}^{\mathrm{B}\bullet}_{\mathrm{B/C}}|_{\mathrm{B}} = \overrightarrow{R}_{\mathrm{B/C}}|_{\mathrm{B}} \vec{\omega}_{\mathrm{B/C}}|_{\mathrm{B}}^{\times} = \tilde{\mathcal{R}} \tilde{\omega}_{\mathrm{B}}^{\times} \quad (19)$$

where $\overrightarrow{R}_{\mathrm{B/C}}$ is the rotation tensor that rotates $\mathrm{F_C}$ into $\mathrm{F_B}$, $\vec{\omega}_{\mathrm{B/C}}$ is the angular velocity of $\mathrm{F_B}$ relative to $\mathrm{F_C}$, and the angular-velocity error $\tilde{\omega}_{\mathrm{B}}$ is defined as

$$\tilde{\omega}_{\mathrm{B}} \triangleq \vec{\omega}_{\mathrm{B/C}}|_{\mathrm{B}} = (\vec{\omega}_{\mathrm{B/I}} - \vec{\omega}_{\mathrm{C/I}})|_{\mathrm{B}} = \omega_{\mathrm{B}} - \tilde{\mathcal{R}}^{\mathrm{T}} \omega_{\mathrm{C}} \quad (20)$$

B. Performance Variable

The objective of the attitude control problem is to align $\mathrm{F_B}$ with the attitude-command frame $\mathrm{F_C}$. To follow attitude commands, a performance variable z is defined and used for adaptive control. A vector representation of the attitude error $\tilde{\mathcal{R}}$ in Eq. (18) is given by

$$S \triangleq \sum_{i=1}^{3} a_i (\tilde{\mathcal{R}}^{\mathrm{T}} e_i) \times e_i = \begin{bmatrix} a_3\tilde{\mathcal{R}}_{32} - a_2\tilde{\mathcal{R}}_{23} \\ a_1\tilde{\mathcal{R}}_{13} - a_3\tilde{\mathcal{R}}_{31} \\ a_2\tilde{\mathcal{R}}_{21} - a_1\tilde{\mathcal{R}}_{12} \end{bmatrix} \in \mathbb{R}^3 \quad (21)$$

where a_1, a_2, and a_3 are real numbers. Note that S depends on the off-diagonal entries of the error matrix $\tilde{\mathcal{R}}$ in Eq. (19).

Lemma 1: Assume that a_1, a_2, and a_3 are distinct, positive numbers. Then, $S = 0$ if, and only if,

$$\tilde{\mathcal{R}} \in \{I_3, \mathrm{diag}(1,-1,1), \mathrm{diag}(-1,1,1), \mathrm{diag}(1,1,-1)\}$$

Proof: See lemma 3 of Ref. [38]. □

Lemma 1 shows that using S as the sole metric of attitude error gives rise to three spurious attitude equilibria. These equilibria can be removed by considering the additional attitude-error metric

$$s \triangleq \mathrm{trace}(A - A\tilde{\mathcal{R}}) = a_1(1 - \tilde{\mathcal{R}}_{11}) + a_2(1 - \tilde{\mathcal{R}}_{22}) + a_3(1 - \tilde{\mathcal{R}}_{33}) \quad (22)$$

where the attitude parameter matrix $A \triangleq \mathrm{diag}(a_1, a_2, a_3)$ is positive definite; and $\tilde{\mathcal{R}}_{11}$, $\tilde{\mathcal{R}}_{22}$, and $\tilde{\mathcal{R}}_{33}$ are the diagonal entries of $\tilde{\mathcal{R}}$. In contrast to S, which depends on the off-diagonal entries of $\tilde{\mathcal{R}}$, the error metric s depends on the diagonal entries of $\tilde{\mathcal{R}}$. The following result is needed.

Lemma 2: For all $i, j \in \{1, 2, 3\}$, the (i, j) entry R_{ij} of a rotation matrix R satisfies $|R_{ij}| \leq 1$.

Proof: See fact 4.13.14 of Ref. [46]. □

The following result shows that S and s can be used together to ensure $\tilde{\mathcal{R}} = I_3$.

Proposition 1: Assume that a_1, a_2, and a_3 are distinct, positive numbers. Then, $S = 0$ and $s = 0$ if, and only if, $\tilde{\mathcal{R}} = I_3$.

Proof: Sufficiency is immediate. To prove necessity, note that $s = 0$ implies that

$$a_1(1 - \tilde{\mathcal{R}}_{11}) + a_2(1 - \tilde{\mathcal{R}}_{22}) + a_3(1 - \tilde{\mathcal{R}}_{33}) = \mathrm{trace}(A - A\tilde{\mathcal{R}}) = 0$$

Lemma 2 implies that, for $i = 1, 2, 3$, $a_i(1 - \tilde{\mathcal{R}}_{ii}) \geq 0$, and thus $a_1(1 - \tilde{\mathcal{R}}_{11}) = a_2(1 - \tilde{\mathcal{R}}_{22}) = a_3(1 - \tilde{\mathcal{R}}_{33}) = 0$.

Because a_1, a_2, and a_3 are positive, it follows that $\tilde{\mathcal{R}}_{11} = \tilde{\mathcal{R}}_{22} = \tilde{\mathcal{R}}_{33} = 1$. Because, by Lemma 1, $\tilde{\mathcal{R}}$ is diagonal, it follows that $\tilde{\mathcal{R}} = I_3$. □

To apply RCAC to attitude control, Lemma 1 and Proposition 1 are used to define the performance variable z by

$$z \triangleq \begin{bmatrix} \tilde{\omega}_{\mathrm{B}} \\ S \\ s \end{bmatrix} \in \mathbb{R}^7 \tag{23}$$

where $\tilde{\omega}_{\mathrm{B}}$ is the angular-velocity error defined by Eq. (20).

Proposition 2: Assume that a_1, a_2, and a_3 are distinct, positive numbers. Then, $z = 0$ if, and only if, $\omega_{\mathrm{B}} = \omega_{\mathrm{C}}$ and $\mathcal{R}_{\mathrm{B/I}} = \mathcal{R}_{\mathrm{C/I}}$.

Proof: For necessity, assume that $z = 0$. Then, $S = 0$, $s = 0$, and Proposition 1 imply that $\tilde{\mathcal{R}} = I_3$. Therefore, Eq. (18) yields $\mathcal{R}_{\mathrm{B/I}} = \mathcal{R}_{\mathrm{C/I}}\tilde{\mathcal{R}} = \mathcal{R}_{\mathrm{C/I}}$. If, in addition, $\tilde{\omega}_{\mathrm{B}} = 0$, then $\omega_{\mathrm{B}} = \tilde{\mathcal{R}}^{\mathrm{T}}\omega_{\mathrm{C}} + \tilde{\omega}_{\mathrm{B}} = \omega_{\mathrm{C}}$. Thus, $\mathcal{R}_{\mathrm{B/I}} = \mathcal{R}_{\mathrm{C/I}}$ and $\omega_{\mathrm{B}} = \omega_{\mathrm{C}}$.

To prove sufficiency, assume that $\mathcal{R}_{\mathrm{C/I}} = \mathcal{R}_{\mathrm{B/I}}$. Then, Eq. (18) implies $\tilde{\mathcal{R}} = I_3$. Thus, Lemma 1 implies that $S = 0$, and Proposition 1 implies that $s = 0$. Next, let $\omega_{\mathrm{B}} = \omega_{\mathrm{C}}$. Then, $\tilde{\omega}_{\mathrm{B}} = \omega_{\mathrm{B}} - \tilde{\mathcal{R}}^{\mathrm{T}}\omega_{\mathrm{C}} = \omega_{\mathrm{B}} - \omega_{\mathrm{C}} = 0$. Thus, $\mathcal{R}_{\mathrm{B/I}} = \mathcal{R}_{\mathrm{C/I}}$ and $\omega_{\mathrm{B}} = \omega_{\mathrm{C}}$ imply that $s = 0$ and $S = \tilde{\omega}_{\mathrm{B}} = 0$. Hence, $z = 0$. □

IV. RCAC Algorithm

This section summarizes the RCAC algorithm as used in the present paper. Because RCAC is a discrete-time control algorithm, it is used to update the coefficients of a discrete-time controller that operates on sampled data. The sampled values of the performance variable $z(t)$ are given by $z_k \triangleq z(kT_{\mathrm{s}})$. Likewise, the continuous-time control input $u(t)$, which is the vector of gimbal rates, is given by a zero-order-hold device. In particular, for all $t \in [kT_{\mathrm{s}}, (k+1)T_{\mathrm{s}})$, it follows that $u(t) = u_k$, where u_k is given by the feedback controller.

A. Controller Structure

Define the strictly proper discrete-time dynamic compensator of order n_c given by

$$u_k = \sum_{i=1}^{n_{\mathrm{c}}} P_{i,k}u_{k-i} + \sum_{i=1}^{n_{\mathrm{c}}} Q_{i,k}z_{k-i} \tag{24}$$

where, for all $i = 1, \ldots, n_{\mathrm{c}}$ and all $k \geq 1$, $P_{i,k} \in \mathbb{R}^{l_u \times l_u}$ and $Q_{i,k} \in \mathbb{R}^{l_u \times l_z}$ are controller coefficient matrices. The control law [Eq. (24)] can be rewritten in regressor form as

$$u_k = \begin{cases} 0, & k < k_w, \\ \Phi_k\Theta_k, & k \geq k_w \end{cases} \tag{25}$$

where the regressor matrix Φ_k, which contains past performance and control data, is defined by

$$\Phi_k \triangleq \begin{bmatrix} u_{k-1} \\ \vdots \\ u_{k-n_{\mathrm{c}}} \\ z_{k-1} \\ \vdots \\ z_{k-n_{\mathrm{c}}} \end{bmatrix}^{\mathrm{T}} \otimes I_{l_u} \in \mathbb{R}^{l_u \times l_\Theta} \tag{26}$$

where $l_\Theta \triangleq l_u n_{\mathrm{c}}(l_u + l_z)$, and k_w is an initial waiting period during which Φ_k is populated with data. The controller coefficient vector Θ_k is defined as

$$\Theta_k \triangleq \mathrm{vec}[P_{1,k} \ \cdots \ P_{n_{\mathrm{c}},k}Q_{1,k} \ \cdots \ Q_{n_{\mathrm{c}},k}]^{\mathrm{T}} \in \mathbb{R}^{l_\Theta} \tag{27}$$

B. Retrospective Performance Variable

The retrospective performance variable is defined by

$$\hat{z}_k(\Theta) \triangleq z_k + G_{\mathrm{f}}(\mathbf{q})[\Phi_k\hat{\Theta} - u_k] \tag{28}$$

where $\hat{\Theta} \in \mathbb{R}^{l_\Theta}$ is the retrospectively optimized controller coefficient vector obtained from the optimization in the following. The updated controller is given by $\Theta_{k+1} = \hat{\Theta}$. As explained in Ref. [36], $G_{\mathrm{f}} \in \mathbb{R}^{l_z \times l_u}$ is a finite-impulse response filter that contains the essential plant modeling information, and $\mathbf{q}$ is the forward shift operator. For linear single-input single-output systems, G_{f} contains modeling information about the leading sign of the numerator, the relative degree, and nonminimum-phase zeros [36]. For linear multi-input multioutput systems, information about the transmission zeros is captured by using Markov parameters of the plant. For nonlinear systems, G_{f} can be constructed by using Markov parameters from of the linearized dynamics [47]. In the present paper, G_{f} is constructed by analyzing the effect of the control input on the performance variable z for the initial gimbal configuration. Additional parameters and weights needed by RCAC are determined from the closed-loop response of a fully nonlinear nominal simulation model; RCAC uses no explicit knowledge of the spacecraft equations of motion. No linearized model of the spacecraft dynamics is needed, created, or used for any purpose in this paper.

C. Retrospective Cost

To update the controller parameter Θ_k, the retrospective cost function is defined by

$$\hat{J}_k(\hat{\Theta}) \triangleq \sum_{i=1}^{k} \hat{z}_i(\hat{\Theta})^{\mathrm{T}}R_z\hat{z}_i(\hat{\Theta}) + (\Phi_i\hat{\Theta})^{\mathrm{T}}R_u\Phi_i\hat{\Theta} + (\hat{\Theta} - \Theta_0)^{\mathrm{T}}R_\Theta(\hat{\Theta} - \Theta_0) \tag{29}$$

where, for all $i \geq 1$, $R_z = \eta_z I_{l_z}$, $R_u = \eta_u I_{l_u}$, and $R_\Theta = \eta_\Theta I_{l_\Theta}$; and η_z, η_u, and η_Θ are positive numbers. As in Ref. [36], the updated controller coefficient matrix Θ_{k+1} that minimizes Eq. (29) is given by recursive least squares. Let $P_0 = R_\Theta^{-1}$ and, for all $k \geq 1$, let Θ_{k+1} be the unique global minimizer of the retrospective cost function [Eq. (29)]. Then, Θ_{k+1} is given by

$$\Theta_{k+1} = \Theta_k - P_k\Phi_{\mathrm{f},k}^{\mathrm{T}}\Gamma_k^{-1}[\Phi_{f,k}\Theta_k + (R_z + R_u)^{-1}R_z(z_k - u_{\mathrm{f},k})] \tag{30}$$

$$P_{k+1} = P_k - P_k\Phi_{\mathrm{f},k}^{\mathrm{T}}\Gamma_k^{-1}\Phi_{\mathrm{f},k}P_k \tag{31}$$

where $\Phi_{\mathrm{f},k} \triangleq G_{\mathrm{f}}(\mathbf{q})\Phi_k$, $u_{\mathrm{f},k} \triangleq G_{\mathrm{f}}(\mathbf{q})u_k$, and $\Gamma_k \triangleq (R_z + R_u)^{-1} + \Phi_{\mathrm{f},k}P_k\Phi_{\mathrm{f},k}^{\mathrm{T}}$.

V. Construction of G_{f}

A. Pyramidal Arrangement of Four CMGs

Consider a spacecraft actuated by $n = 4$ CMGs mounted in the pyramidal arrangement shown in Fig. 4. Because the CMGs apply a pure torque to the bus, the location of the pyramidal arrangement on the bus is immaterial. The pyramid has a square base, for which the sides define the axes $\hat{\imath}_{\mathrm{B}}$ and $\hat{\jmath}_{\mathrm{B}}$ of the bus. Consequently, the sides of the pyramidal base are aligned with $\hat{\imath}_{\mathrm{B}}$ and $\hat{\jmath}_{\mathrm{B}}$, and β is the angle between a vector orthogonal to each face and the apex direction $\hat{k}_{\mathrm{B}}$. The CMGs are arranged such that, for $i = 1, 2, 3, 4$, each axis $\hat{\jmath}_{\mathrm{G}_i}$ of rotation of gimbal G_i relative to the bus is perpendicular to the corresponding face; each axis $\hat{\imath}_{\mathrm{G}_i}$ of rotation of wheel W_i relative to the gimbal is parallel with the corresponding edge of the base. Therefore, the angular momentum of W_i, which aligns with $\hat{\imath}_{\mathrm{G}_i}$, lies in the plane spanned by the corresponding face. A counterclockwise gimbal angular velocity u_i around $\hat{\jmath}_{\mathrm{G}_i}$ is defined to be positive, and thus $u_i = \dot{\theta}_i$. The initial orientation matrices corresponding to this CMG arrangement are given by

$$\begin{aligned}
\mathcal{O}_1(\theta_1(0)) &= \mathcal{R}\left(\beta - \frac{\pi}{2}, e_1\right)^{\mathrm{T}}\mathcal{R}(\theta_1(0), e_2), \\
\mathcal{O}_2(\theta_2(0)) &= \mathcal{R}\left(\beta - \frac{\pi}{2}, e_2\right)^{\mathrm{T}}\mathcal{R}\left(-\frac{\pi}{2}, e_3\right)^{\mathrm{T}}\mathcal{R}(\theta_2(0), e_2), \\
\mathcal{O}_3(\theta_3(0)) &= \mathcal{R}\left(\frac{\pi}{2} - \beta, e_1\right)^{\mathrm{T}}\mathcal{R}(-\pi, e_3)^{\mathrm{T}}\mathcal{R}(\theta_3(0), e_2), \\
\mathcal{O}_4(\theta_4(0)) &= \mathcal{R}\left(\frac{\pi}{2} - \beta, e_2\right)^{\mathrm{T}}\mathcal{R}\left(\frac{\pi}{2}, e_3\right)^{\mathrm{T}}\mathcal{R}(\theta_4(0), e_2)
\end{aligned} \tag{32}$$

where $\mathcal{R}(\phi, \xi)$ is given by Rodrigues's formula

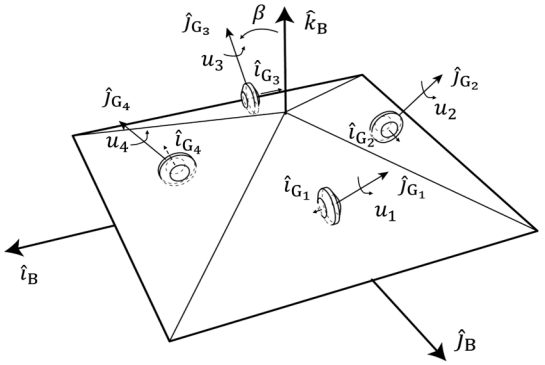

Fig. 4 Pyramidal arrangement of four CMGs.

$$\mathcal{R}(\phi,\xi) = (\cos\phi)I_3 + (1-\cos\phi)\xi\xi^{\mathrm{T}} + (\sin\phi)\xi^{\times} \tag{33}$$

$\xi \in \mathbb{R}^3$ is a unit vector, and $\phi \in (-\pi, \pi]$.

B. Construction of G_f

For the pyramidal arrangement of four CMGs and with the initial gimbal configuration $\theta_1(0) = \theta_2(0) = \theta_3(0) = \theta_4(0) = 0$, note that this initial gimbal configuration is nonsingular in the sense that there is no constraint on the achievable torque vectors. Also, u_i changes the direction of the angular momentum of W_i, which produces the gimbal torque τ_{G_i}. For gimbal G_i, τ_{G_i} for the initial gimbal configuration lies in a face of the pyramid, orthogonal to $\hat{\imath}_{G_i}$, as shown in Fig. 5. The vector sum of τ_{G_1}, τ_{G_2}, τ_{G_3}, and τ_{G_4} is τ_{CMG} in Eq. (12).

For the initial gimbal configuration $\theta_1(0) = \theta_2(0) = \theta_3(0) = \theta_4(0) = 0$, Fig. 5 shows that τ_{G_1} can be decomposed in the directions $\hat{\jmath}_B$ and $-\hat{k}_B$; τ_{G_2} can be decomposed in the directions $-\hat{\imath}_B$ and $-\hat{k}_B$; τ_{G_3} can be decomposed in the directions $-\hat{\jmath}_B$ and $-\hat{k}_B$; and τ_{G_4} can be decomposed in the directions $\hat{\imath}_B$ and $-\hat{k}_B$. Based on these observations, G_f is chosen to be

$$G_f(\mathbf{q}) = \frac{1}{\mathbf{q}}H \tag{34}$$

where H captures the effect of the gimbal control input on the performance variable z for the given initial gimbal configuration. H is thus given by

$$H = -\begin{bmatrix} 0 & -1 & 0 & 1 \\ 1 & 0 & -1 & 0 \\ -1 & -1 & -1 & -1 \\ 0 & -1 & 0 & 1 \\ 1 & 0 & -1 & 0 \\ -1 & -1 & -1 & -1 \\ 0 & 0 & 0 & 0 \end{bmatrix} \tag{35}$$

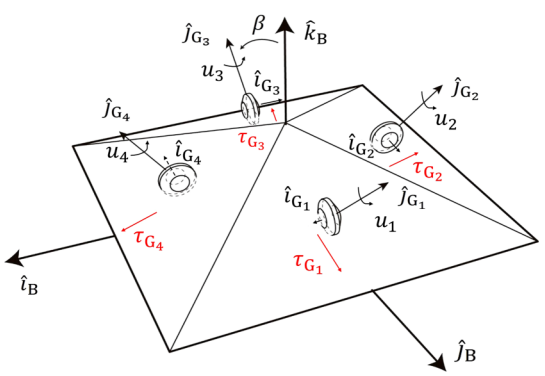

Fig. 5 Gimbal torque directions for the initial gimbal configuration.

where the leading minus sign is due to the error junction in Fig. 2. For all numerical examples, G_f is fixed and given by Eq. (34), with H given by Eq. (35).

VI. Numerical Examples

A. Numerical Integration of the Sampled-Data Dynamics

RCAC updates the coefficients of the discrete-time controller [Eq. (24)] for which the output u_k is applied to the continuous-time spacecraft dynamics using a zero-order-hold device. The closed-loop system thus has sampled-data dynamics. To capture the intersample dynamics, the MATLAB function ODE45 is used with a variable step size in order to ensure integration accuracy. In addition, ODE45 is applied in each sampling interval $t \in [kT_s, (k+1)T_s)$ with a fixed integration interval of length T_s in order to ensure that the integration is synchronous with updates of the zero-order-hold control signal.

B. Simulation Performance Metric

The accuracy of RCAC is assessed by using the eigenangle ϕ_{eig} of $\tilde{\mathcal{R}}$ as the error metric, where

$$\phi_{eig} \triangleq \cos^{-1}\frac{1}{2}(\mathrm{tr}\tilde{\mathcal{R}} - 1) \tag{36}$$

The eigenangle ϕ_{eig} is the rotation angle around the eigenaxis that rotates $\mathcal{R}_{B/I}(t)$ to the attitude command $\mathcal{R}_{C/I}(t)$. Using Rodrigues's formula [Eq. (33)], $\mathcal{R}_{C/I}$ can be represented by the commanded eigenangle ϕ_C and the commanded eigenaxis ξ_C resolved in F_I. The transient performance is given by the settling time T_s to be the time needed to bring and maintain ϕ_{eig} within a specified bound ϕ_∞ for all $t \geq T_s$,

$$\phi_{eig}(t) \leq \phi_\infty \tag{37}$$

where $\phi_\infty \triangleq 3$ deg. The final error metric is the value of $\phi_{eig}(t)$ averaged over the last 1 s of simulation.

For all examples, the controller coefficients are initialized at $\Theta(0) = 0$. This choice reflects the absence of prior modeling information. If additional modeling information is available, this information may be advantageous for initializing $\Theta(0)$.

C. Nominal-Model Tuning

Nominal-simulation tuning refers to the tuning of RCAC based on simulation of a nominal model. Instead of attempting to identify the system, the simulation is run a small number of times to tune the parameters of RCAC to the nominal simulation. No attempt is made to optimize the response.

To demonstrate this approach, consider a rest-to-rest maneuver, where the spacecraft is assumed to be initially at rest with $\mathcal{R}_{B/I}(0) = I_3$, $\omega_B(0) = 0$, and $u(0) = 0$; and the attitude and angular-velocity commands are given by $\mathcal{R}_{B/I} = \mathcal{R}_{C/I}$ and $\omega_C = 0$. For nominal-model tuning, the commanded eigenangle is $\phi_C = -150$ deg around the commanded eigenaxis $\xi_C = [1 \quad 1 \quad 1]^{\mathrm{T}}$.

The nominal simulation model assumes the following parameter values. The bus inertia matrix is $J_B = \mathrm{diag}(10, 25/3, 5)$ kg · m^2, which implies that F_B is a principal-axis frame for the bus inertia of the nominal simulation model. For $i = 1, 2, 3, 4$, the wheel inertia is $J_i = \mathrm{diag}(0.02, 0.012, 0.012)$ kg · m^2, the wheel mass is $m_i = 0.001$ kg, and the wheel spin speed is $\nu_i = 600$ rad/s. The gimbal positions are $r_1 = [0 \quad 0.1 \quad 0]^{\mathrm{T}}$ m, $r_2 = [-0.1 \quad 0 \quad 0]^{\mathrm{T}}$ m, $r_3 = [0 \quad -0.1 \quad 0]^{\mathrm{T}}$ m, and $r_4 = [0.1 \quad 0 \quad 0]^{\mathrm{T}}$ m. The pyramidal face angle is $\beta = 54$ deg, and the initial gimbal angles are $\theta_1(0) = \theta_2(0) = \theta_3(0) = \theta_4(0) = 0$ deg. The attitude parameter matrix is chosen to be $A = \mathrm{diag}(1, 2, 3)$.

Nominal-model tuning with the sample time of 0.1 s yields the parameter choices $n_c = 2$, $\eta_z = \eta_u = 1$, $\eta_\Theta = 0.01$, and $k_w = 5$ steps. These values reflect the fact that the nominal-model tuning is limited to a small number of runs with no attempt to optimize the response. With these tuning parameters, the settling time is $T_s = 12.3$ s with the final error of 1.1×10^{-7} deg.

D. Perturbed-Model Testing

In perturbed-model testing, the parameters and weights obtained under nominal-model tuning are fixed, and the robustness and performance of RCAC are evaluated through simulations based on perturbations of the nominal model. These perturbations are chosen to reflect off-nominal conditions of the model, commands, sensor noise, actuator misalignment, and the singularities that can potentially occur in real-world operations.

1. *Rest-to-Rest Rotation Maneuvers with Sensor Noise*

The commanded eigenangle ϕ_C varies from -180 to 180 deg around the commanded eigenaxes $[1 \quad 1 \quad 1]^{\mathrm{T}}$, $[1 \quad 0 \quad 0]^{\mathrm{T}}$, $[0 \quad 1 \quad 0]^{\mathrm{T}}$, and $[0 \quad 0 \quad 1]^{\mathrm{T}}$. Zero-mean Gaussian white noise with a covariance of $0.01I_3$ is assumed to corrupt the sensors that measure the angular velocity ω_{B} of the bus. Figure 6 shows the settling time and error at 50 s.

2. *Rest-to-Rest Rotation Maneuver*

The commanded attitude maneuver is a rest-to-rest rotation around the eigenaxis $\xi_C = [0 \quad 1 \quad 0]^{\mathrm{T}}$, beginning at 0.5 s, ending at 15 s, and with the constant rate of 0.18 rad/s. Figure 7a compares the actual attitude to the attitude command; and Fig. 7b shows the corresponding eigenangle error.

3. *Robustness to Diagonal Perturbations of the Bus Inertia Matrix*

The robustness of RCAC to uncertainty in the principal moments of inertia is assessed by considering a collection of diagonal bus inertia matrices $J_{\mathrm{B}} = \mathrm{diag}(\lambda_1, \lambda_2, \lambda_3)$. Figure 1 in Ref. [48] provided a convenient classification of all possible principal moments of inertia in relation to the underlying geometry. In particular, the triangular shaded region shows all feasible values of λ_2 and λ_3 in terms of the largest principal moment of inertia λ_1. The vertices of the region correspond to a sphere, a thin disk, and a thin pencil. For additional details, see Ref. [48].

The attitude command is to rotate -150 deg around $\xi_C = [1 \quad 1 \quad 1]^{\mathrm{T}}$. The unknown bus inertia matrix $\mathrm{diag}(\lambda_1, \lambda_2, \lambda_3)$ is assumed to be diagonal and is given by the 422 points of the triangular regions in Fig. 8, which correspond to the shaded triangular region in figure 1 in Ref. [48]. Figure 8 shows the settling time for each bus inertia matrix. For all simulations, the measurements of ω_{B} are corrupted by zero-mean Gaussian white sensor noise with covariance of $0.01I_3$.

4. *Robustness to Off-Diagonal Perturbations of the Bus Inertia Matrix*

As shown in Fig. 9, the rotated bus inertia matrix $J_{\mathrm{B,rot}}$ is defined as

$$J_{\mathrm{B,rot}} \triangleq \mathcal{R}(\theta, e)^{\mathrm{T}} J_{\mathrm{B}} \mathcal{R}(\theta, e) \tag{38}$$

where $\mathcal{R}(\theta, e)$ is given by Rodrigues's formula [Eq. (33)] with $e = [1 \quad 1 \quad 1]^{\mathrm{T}}$. Consequently, $\mathrm{F_B}$ is no longer a principal-axis frame of the bus. For the simulation, zero-mean Gaussian white noise with covariance of $0.01I_3$ is assumed to corrupt the measurements of ω_{B}. The end time for all simulations in Fig. 9 is 300 s. The nonmonotonic trend suggests a complex relationship between the initial gimbal configuration and the rotated inertia matrix.

5. *Approximate Singularity Passthrough*

Rerunning the 422 maneuvers tested in Fig. 8 in the absence of sensor noise, there are 32 times at which the minimum singular value of B_{CMG} is less than 0.1. Of these 32 cases, the smallest minimum singular value of B_{CMG} occurs for the inertia matrix $\mathrm{diag}(30, 22, 15)$ kg $\cdot$ m^2 shown in Fig. 10. In particular, Fig. 10b shows that, at the time resolution of 0.1 s of the numerical integration, an approximate singularity passthrough occurs at a time of 31.2 s, when the minimum singular value of B_{CMG} reaches its smallest value, namely, 0.0313. A closer approach to a singularity occurs in Fig. 11 where, at a time of 27.5 s, the minimum singular value reaches 0.0038 without any adverse effect. Because the control input matrix B_{CMG} is time dependent, rank-deficient conditions tend to hold at only isolated points, and thus the use of requested gimbal rates is able to overcome singularities encountered instantaneously during attitude command following.

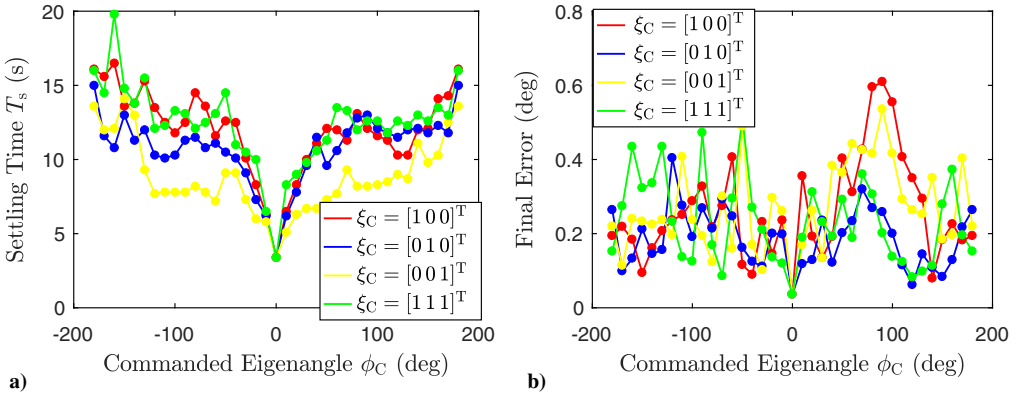

Fig. 6 Plots of a) settling time T_s and b) error at 50 s.

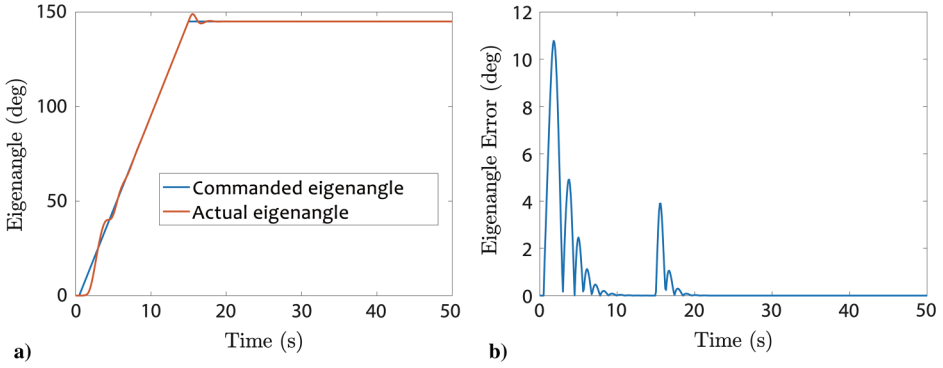

Fig. 7 Plots of a) commanded and actual eigenangles, and b) eigenangle error.

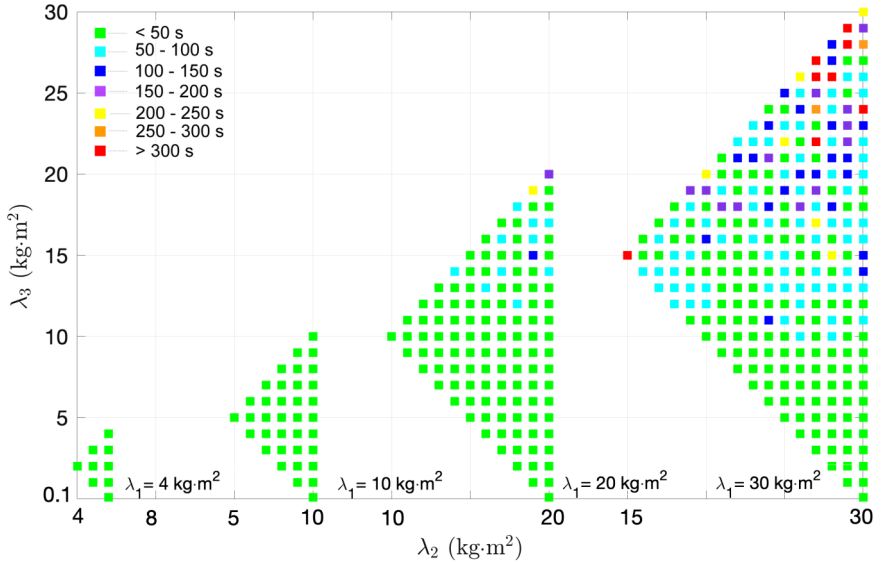

Fig. 8 Settling time T_s as a function of the bus inertia matrix $\mathrm{diag}(\lambda_1, \lambda_2, \lambda_3)$ for λ_2 in the ranges [4, 8], [5, 10], [10, 20], and [15, 30] kg · m^2.

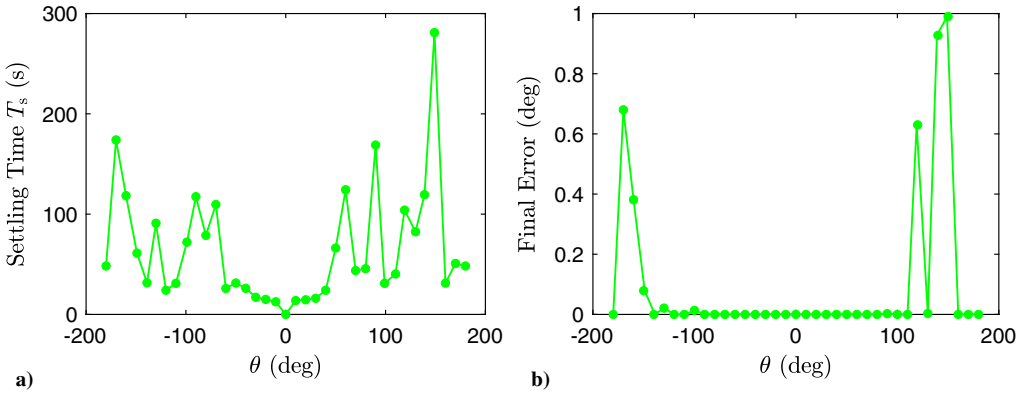

Fig. 9 Plots of a) settling time T_s, and b) error at 300 s.

6. Escape from an Initial Gimbal-Lock Singularity

To consider the case of an exact, impassable gimbal singularity, the initial gimbal configuration is chosen to be different from the initial gimbal configuration considered in the previous subsections; however, no change is made to H defined by Eq. (35) for $\theta(0) = [0 \quad 0 \quad 0 \quad 0]$ deg. The attitude command is to rotate the spacecraft −150 deg around the eigenaxis $[0 \quad 0 \quad 1]^{\mathrm{T}}$. Letting $\theta(0) = [-90 \quad 90 \quad -90 \quad 90]$ deg, no torque can be generated in the direction of $\hat{k}_{\mathrm{B}}$. Therefore, the initial torque required for the commanded attitude maneuver is not in the range of B_{CMG}, and thus it is a singular direction of the initial gimbal configuration. Consequently, it is impossible for the spacecraft to initially rotate in the commanded direction; this case represents an impassable singularity corresponding to gimbal lock.

The minimum singular value of B_{CMG} during the first five steps is 1.4×10^{-15} (due to numerical roundoff) because RCAC must wait five steps due to Eq. (25), where $k_W = 5$. The minimum singular value of B_{CMG} at $t = 0.6$ s is 0.24. As shown in Fig. 11b, RCAC initially takes an indirect route in following the attitude command in order to escape from the gimbal lock. For the same initially singular gimbal configuration, a nonsingular torque request is used in Ref. [24] to escape the singularity.

To assess the performance degradation due to the initial gimbal singularity, RCAC is applied to the spacecraft with thruster actuation only: that is, without CMGs. Based on the response of the nominal model, H is redefined to be $H = [-I_3 \quad -I_3 \quad 0_{3\times 1}]^{\mathrm{T}}$; all of the remaining parameters and weights of RCAC are the same as in the case of CMGs. Using RCAC, the spacecraft with thrusters is simulated with the same bus inertia, initial conditions, and attitude command as the spacecraft with CMGs. Figure 11b shows that, under thruster control, the attitude of the spacecraft generally decreases, where the oscillations indicate that the attitude overshoots the setpoint but eventually damps out. In contrast, due to the initial gimbal-lock singularity, RCAC drives the attitude in the opposite direction, as evidenced by the increasing eigenangle. At a time of 330 s, however, the eigenangle decreases monotonically and rapidly to the attitude command, which it reaches at a time of 357.8 s with a final error of 3.88×10^{-5} deg.

7. Robustness to Sensor/Actuator Misalignment

In all previous simulations, the attitude sensors are assumed to be perfectly aligned with the pyramidal CMGs. In particular, the sensing axes are assumed to be exactly aligned with the axes of the bus frame $\mathrm{F_B}$, which also defines the directions of the CMGs. However, sensor/actuator misalignment can occur in practice; in which case, the sensing axes may be different from the axes that define the gimbal directions [49,50]. This misalignment is assumed to be unknown to RCAC, and it is of interest to determine the effect of the sensor/actuator misalignment on the attitude error.

To determine the performance degradation due to sensor/actuator misalignment, it is assumed, as in previous sections, that the base of the CMG pyramid is aligned with the axes of the bus frame $\mathrm{F_B}$. However, the sensors, which are misaligned with the CMGs, are aligned with a rotated frame $\mathrm{F'_B}$. The rotation tensor $\overrightarrow{R}_{\mathrm{B'/B}}$ thus determines the alignment of the CMGs relative to the attitude sensors; this rotation tensor is assumed to be unknown to RCAC. In

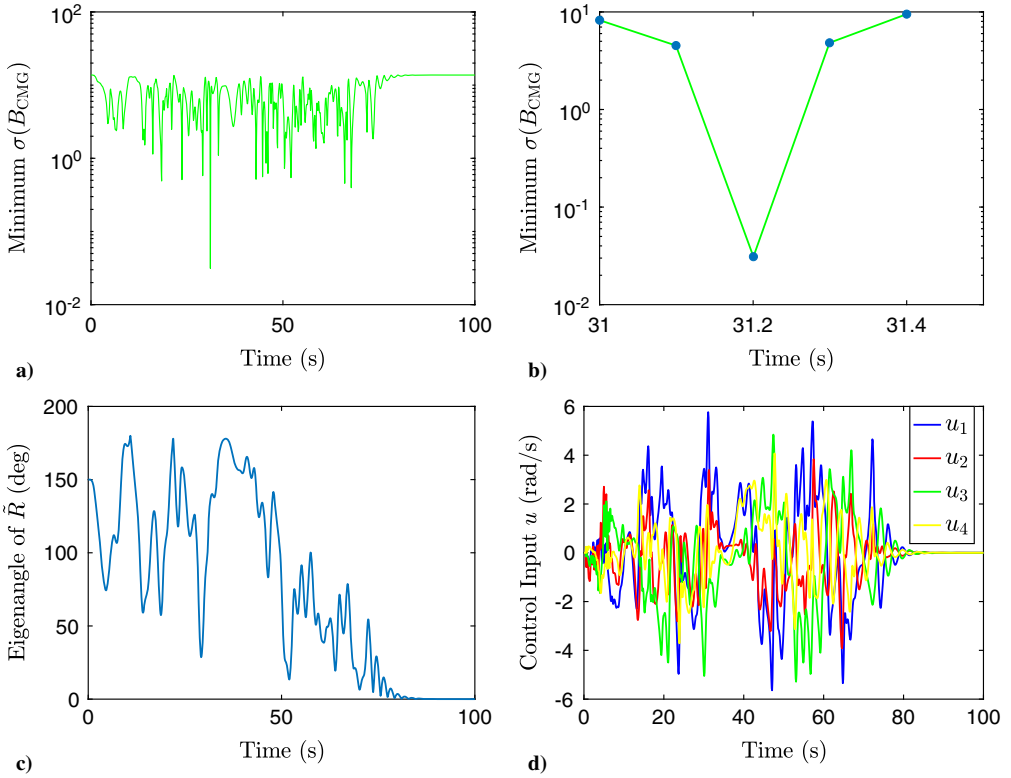

Fig. 10 Plots of a) minimum singular value, b) approximate singularity passthrough between 31.0 and 31.4 s, c) eigenangle error, and d) control input u.

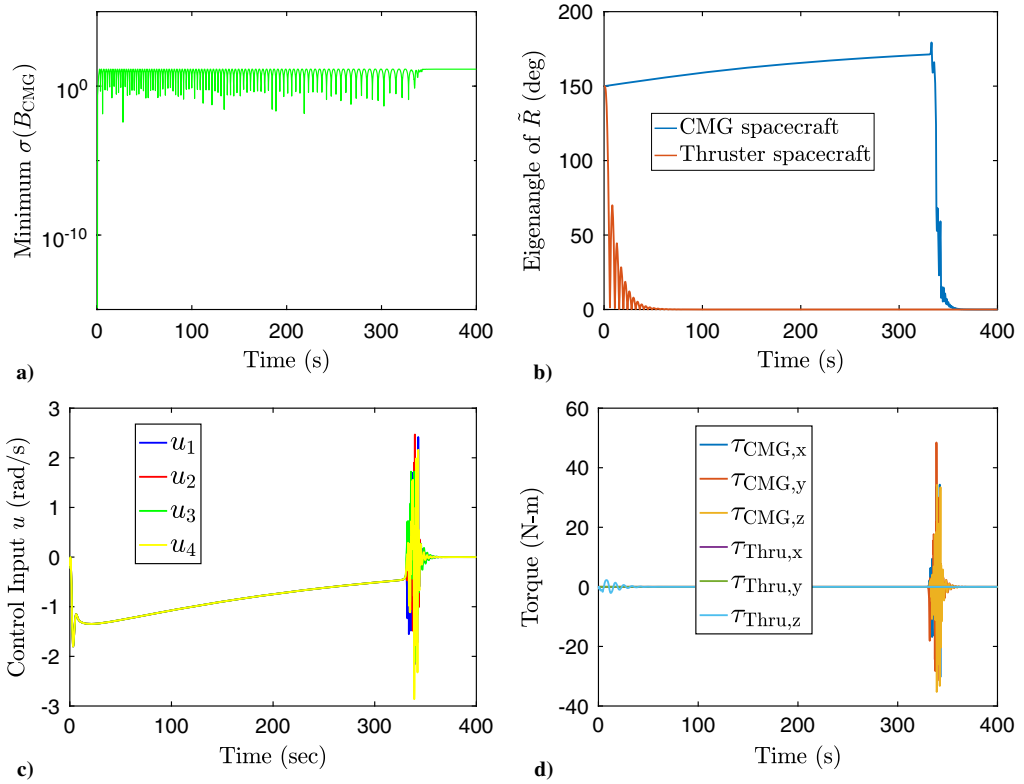

Fig. 11 Plots of a) minimum singular value, b) eigenangle error, c) gimbal-rate control input u, and d) CMG and thruster torques.

the absence of misalignment, $\overrightarrow{R}_{\mathrm{B}'/\mathrm{B}}$ is the identity second-order tensor.

Because the attitude error is determined by the sensor measurements, the goal is to determine the performance degradation due to the misalignment between $\mathrm{F_B}$ and $\mathrm{F_B'}$. Note that, due to the misalignment, Eq. (8) is replaced by

$$\mathcal{O}_{i'} \triangleq \mathcal{O}_{\mathrm{B}'/\mathrm{G}_i} = \overrightarrow{R}_{\mathrm{G}_i/\mathrm{B}'}|_{\mathrm{B}'} = \mathcal{O}_{\mathrm{B}'/\mathrm{B}}\mathcal{O}_{\mathrm{B}/\mathrm{G}_i} = \mathcal{R}(\theta', e')^{\mathrm{T}}\mathcal{O}_{\mathrm{B}/\mathrm{G}_i} \tag{39}$$

where θ' and e' are the misalignment eigenangle and misalignment from $\mathrm{F_B}$ to $\mathrm{F_{B'}}$. The commanded attitude maneuver is to rotate

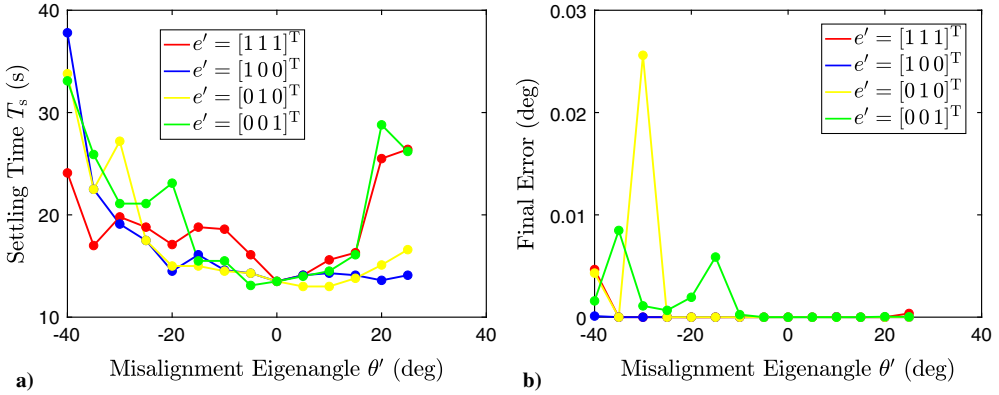

Fig. 12 Plots of a) settling time T_s, and b) error at 50 s.

-150 deg around $\xi_C = [1 \quad 1 \quad 1]^{\mathrm{T}}$. The misalignment eigenangle θ' varies from -40 to 25 deg around four choices of the eigenaxis e', namely, $[1 \quad 1 \quad 1]^{\mathrm{T}}$, $[1 \quad 0 \quad 0]^{\mathrm{T}}$, $[0 \quad 1 \quad 0]^{\mathrm{T}}$, and $[0 \quad 0 \quad 1]^{\mathrm{T}}$. Figure 12 shows the settling time and error at 50 s.

VII. Conclusions

Adaptive control of a rigid spacecraft controlled by a pyramidal arrangement of four single-gimbal constant-speed CMGs was considered. Retrospective cost adaptive control was used with gimbal-rate-requested CMGs; no torque-steering law was used. The RCAC implementation was based on a target model involving a single Markov parameter corresponding to the initial gimbal configuration. The parameters and weights for RCAC were based on a nominal simulation; no explicit knowledge of the nonlinear equations of motion was used by the adaptive controller.

Numerical simulations with a perturbed model showed that the adaptive controller is robust to large variations in the spacecraft inertia in the presence of gyroscope noise. The performance across these variations shows the robustness of RCAC to the choice of the target model. The controller was able to escape from an initial gimbal-lock singularity and not suffer from close approach to a gimbal singularity.

An open problem is to consider the effect of the gimbal angular acceleration $\dot{u}$ on the closed-loop performance. Although this term is typically neglected in the analysis of torque-steering laws ([4] p. 80), its effect on the performance of CMG-controlled spacecraft remains to be investigated.

Appendix: Derivation of the Equations of Motion

Assumptions 1, 2, and 3 imply that the center of mass c of the spacecraft is fixed in B. Therefore, the angular momentum $\vec{H}_{\mathrm{B/c/I}}$ of B relative to c with respect to $\mathrm{F_I}$ is given by

$$\vec{H}_{\mathrm{B/c/I}} = \overrightarrow{J}_{\mathrm{B/c}}\vec{\omega}_{\mathrm{B/I}} \tag{A1}$$

where $\overrightarrow{J}_{\mathrm{B/c}}$ is the inertia tensor of the bus relative to c. The angular momentum $\vec{H}_{\mathrm{W}_i\mathrm{/c/I}}$ of W_i relative to c with respect to $\mathrm{F_I}$ is given by

$$\vec{H}_{\mathrm{W}_i\mathrm{/c/I}} = \vec{H}_{\mathrm{W}_i\mathrm{/c}_i\mathrm{/I}} + \vec{r}_{\mathrm{c}_i\mathrm{/c}} \times m_i \overset{\mathrm{I}\bullet}{\vec{r}}_{\mathrm{c}_i\mathrm{/c}} \tag{A2}$$

where $\vec{H}_{\mathrm{W}_i\mathrm{/c}_i\mathrm{/I}}$ is the angular momentum of W_i relative to its center of mass c_i with respect to $\mathrm{F_I}$, $\vec{r}_{\mathrm{c}_i\mathrm{/c}}$ is the position of c_i relative to c, m_i is the mass of W_i, and I$\bullet$ denotes the derivative with respect to $\mathrm{F_I}$. Applying the transport theorem to $\overset{\mathrm{I}\bullet}{\vec{r}}_{\mathrm{c}_i\mathrm{/c}}$ in Eq. (A2) yields

$$\vec{H}_{\mathrm{W}_i\mathrm{/c/I}} = \vec{H}_{\mathrm{W}_i\mathrm{/c}_i\mathrm{/I}} + \vec{r}_{\mathrm{c}_i\mathrm{/c}} \times m_i(\overset{\mathrm{B}\bullet}{\vec{r}}_{\mathrm{c}_i\mathrm{/c}} + \vec{\omega}_{\mathrm{B/I}} \times \vec{r}_{\mathrm{c}_i\mathrm{/c}}) \tag{A3}$$

where B$\bullet$ denotes the derivative with respect to $\mathrm{F_B}$. Because c and c_i are fixed in the bus, it follows that $\overset{\mathrm{B}\bullet}{\vec{r}}_{\mathrm{c}_i\mathrm{/c}} = 0$. Therefore,

$$\begin{aligned}\vec{H}_{\mathrm{W}_i\mathrm{/c/I}} &= \vec{H}_{\mathrm{W}_i\mathrm{/c}_i\mathrm{/I}} + m_i \vec{r}_{\mathrm{c}_i\mathrm{/c}} \times (\vec{\omega}_{\mathrm{B/I}} \times \vec{r}_{\mathrm{c}_i\mathrm{/c}}) \\ &= \vec{H}_{\mathrm{W}_i\mathrm{/c}_i\mathrm{/I}} - m_i \vec{r}^{\times 2}_{\mathrm{c}_i\mathrm{/c}}\vec{\omega}_{\mathrm{B/I}}\end{aligned} \tag{A4}$$

Because, by Assumption 3, c_i is fixed in W_i, $\vec{H}_{\mathrm{W}_i\mathrm{/c}_i\mathrm{/I}}$ is given by

$$\vec{H}_{\mathrm{W}_i\mathrm{/c}_i\mathrm{/I}} = \overrightarrow{J}_{\mathrm{W}_i\mathrm{/c}_i}\vec{\omega}_{\mathrm{W}_i\mathrm{/I}} \tag{A5}$$

where $\overrightarrow{J}_{\mathrm{W}_i\mathrm{/c}_i}$ is the inertia tensor of W_i relative to c_i, and $\vec{\omega}_{\mathrm{W}_i\mathrm{/I}}$ is the angular velocity of $\mathrm{F_{W_i}}$ relative to $\mathrm{F_I}$. Expanding $\vec{\omega}_{\mathrm{W}_i\mathrm{/I}}$ in Eq. (A5) yields

$$\vec{H}_{\mathrm{W}_i\mathrm{/c}_i\mathrm{/I}} = \overrightarrow{J}_{\mathrm{W}_i\mathrm{/c}_i}(\vec{\omega}_{\mathrm{W}_i\mathrm{/B}} + \vec{\omega}_{\mathrm{B/I}}) \tag{A6}$$

$$= \overrightarrow{J}_{\mathrm{W}_i\mathrm{/c}_i}(\vec{\omega}_{\mathrm{W}_i\mathrm{/G}_i} + \vec{u}_i + \vec{\omega}_{\mathrm{B/I}}) \tag{A7}$$

where, by Assumption 7, the control vector $\vec{u}_i$ for CMG_i is the angular velocity of $\mathrm{F_{G_i}}$ relative to $\mathrm{F_B}$; that is,

$$\vec{u}_i \triangleq \vec{\omega}_{\mathrm{G}_i\mathrm{/B}} \tag{A8}$$

Substituting Eq. (A7) into Eq. (A4) yields

$$\vec{H}_{\mathrm{W}_i\mathrm{/c/I}} = \overrightarrow{J}_{\mathrm{W}_i\mathrm{/c}_i}(\vec{\omega}_{\mathrm{W}_i\mathrm{/G}_i} + \vec{u}_i) + \overrightarrow{J}_{\mathrm{W}_i\mathrm{/c}}\vec{\omega}_{\mathrm{B/I}} \tag{A9}$$

where, by the parallel axis theorem,

$$\overrightarrow{J}_{\mathrm{W}_i\mathrm{/c}} = \overrightarrow{J}_{\mathrm{W}_i\mathrm{/c}_i} - m_i \vec{r}^{\times 2}_{\mathrm{c}_i\mathrm{/c}} \tag{A10}$$

By Assumption 2, the angular momentum $\vec{H}_{\mathrm{G}_i\mathrm{/c/I}}$ of G_i relative to c with respect to $\mathrm{F_I}$ is zero. Therefore, the angular momentum $H_{\mathrm{SC/c/I}}$ of the spacecraft relative to c with respect to $\mathrm{F_I}$ is given by

$$\vec{H}_{\mathrm{SC/c/I}} = \vec{H}_{\mathrm{B/c/I}} + \sum_{i=1}^{n} \vec{H}_{\mathrm{W}_i\mathrm{/c/I}} \tag{A11}$$

Using Eqs. (A1) and (A9), Eq. (A11) can be rewritten as

$$\vec{H}_{\mathrm{SC/c/I}} = \overrightarrow{J}_{\mathrm{SC/c}}\vec{\omega}_{\mathrm{B/I}} + \sum_{i=1}^{n} \overrightarrow{J}_{\mathrm{W}_i\mathrm{/c}_i}(\vec{\omega}_{\mathrm{W}_i\mathrm{/G}_i} + \vec{u}_i) \tag{A12}$$

where the inertia tensor of the spacecraft relative to its center of mass is given by

$$\overrightarrow{J}_{\mathrm{SC/c}} = \overrightarrow{J}_{\mathrm{B/c}} + \sum_{i=1}^{n} \overrightarrow{J}_{\mathrm{W}_i\mathrm{/c}} \tag{A13}$$

A. Dynamics

A.1. Euler's Equation for the Angular Momentum of the Spacecraft

Applying the angular momentum theorem to the spacecraft yields

$$\overset{\mathrm{I}\bullet}{\vec{H}}_{\mathrm{SC/c/I}} = \vec{M}_{\mathrm{SC}} \tag{A14}$$

where $\vec{M}_{\mathrm{SC}}$ is the sum of all external torques acting on the spacecraft. Applying the transport theorem to the left side of Eq. (A14) yields

$$\overset{\mathrm{I}\bullet}{\vec{H}}_{\mathrm{SC/c/I}} = \overset{\mathrm{B}\bullet}{\vec{H}}_{\mathrm{SC/c/I}} + \vec{\omega}_{\mathrm{B/I}} \times \vec{H}_{\mathrm{SC/c/I}} \tag{A15}$$

Hence, Eqs. (A14) and (A15) imply

$$\overset{\mathrm{B}\bullet}{\vec{H}}_{\mathrm{SC/c/I}} + \vec{\omega}_{\mathrm{B/I}} \times \vec{H}_{\mathrm{SC/c/I}} = \vec{M}_{\mathrm{SC}} \tag{A16}$$

which is Euler's equation for the angular momentum of the spacecraft.

A.2. Derivatives of the Wheel Angular Momenta with Respect to $\mathrm{F_B}$

Differentiating Eq. (A11) with respect to $\mathrm{F_B}$ yields

$$\overset{\mathrm{B}\bullet}{\vec{H}}_{\mathrm{SC/c/I}} = \overset{\mathrm{B}\bullet}{\vec{H}}_{\mathrm{B/c/I}} + \sum_{i=1}^{n} \overset{\mathrm{B}\bullet}{\vec{H}}_{\mathrm{W}_i/\mathrm{c/I}} \tag{A17}$$

Because, by Assumption 1, the inertia $\overrightarrow{J}_{\mathrm{B/c}}$ is constant with respect to $\mathrm{F_B}$, differentiating Eq. (A1) with respect to $\mathrm{F_B}$ yields

$$\overset{\mathrm{B}\bullet}{\vec{H}}_{\mathrm{B/c/I}} = \overrightarrow{J}_{\mathrm{B/c}} \overset{\mathrm{B}\bullet}{\vec{\omega}}_{\mathrm{B/I}} \tag{A18}$$

Furthermore, differentiating Eq. (A9) with respect to $\mathrm{F_B}$ and using Eq. (A10) yields

$$\begin{aligned}\overset{\mathrm{B}\bullet}{\vec{H}}_{\mathrm{W}_i/\mathrm{c/I}} &= \overset{\mathrm{B}\bullet}{\overrightarrow{J}}_{\mathrm{W}_i/\mathrm{c}_i}(\vec{\omega}_{\mathrm{W}_i/\mathrm{G}_i} + \vec{u}_i) + \overrightarrow{J}_{\mathrm{W}_i/\mathrm{c}_i}(\overset{\mathrm{B}\bullet}{\vec{\omega}}_{\mathrm{W}_i/\mathrm{G}_i} + \overset{\mathrm{B}\bullet}{\vec{u}}_i) \\ &+ (\overset{\mathrm{B}\bullet}{\overrightarrow{J}}_{\mathrm{W}_i/\mathrm{c}_i} - m_i \overset{\mathrm{B}\bullet}{\overbrace{\vec{r}^{\times 2}_{\mathrm{c}_i/\mathrm{c}}}})\vec{\omega}_{\mathrm{B/I}} + \overrightarrow{J}_{\mathrm{W}_i/\mathrm{c}} \overset{\mathrm{B}\bullet}{\vec{\omega}}_{\mathrm{B/I}}\end{aligned} \tag{A19}$$

Next, using Eq. (A8), the derivative of $\overrightarrow{J}_{\mathrm{W}_i/\mathrm{c}_i}$ with respect to $\mathrm{F_B}$ is given by

$$\begin{aligned}\overset{\mathrm{B}\bullet}{\overrightarrow{J}}_{\mathrm{W}_i/\mathrm{c}_i} &= \overset{\mathrm{G}_i\bullet}{\overrightarrow{J}}_{\mathrm{W}_i/\mathrm{c}_i} + \vec{\omega}^{\times}_{\mathrm{G}_i/\mathrm{B}} \overrightarrow{J}_{\mathrm{W}_i/\mathrm{c}_i} - \overrightarrow{J}_{\mathrm{W}_i/\mathrm{c}_i} \vec{\omega}^{\times}_{\mathrm{G}_i/\mathrm{B}} \\ &= \vec{u}_i^{\times} \overrightarrow{J}_{\mathrm{W}_i/\mathrm{c}_i} - \overrightarrow{J}_{\mathrm{W}_i/\mathrm{c}_i} \vec{u}_i^{\times}\end{aligned} \tag{A20}$$

where

$$\overset{\mathrm{G}_i\bullet}{\overrightarrow{J}}_{\mathrm{W}_i/\mathrm{c}_i} = 0$$

due to Assumptions 1, 5, and 6. Furthermore, Assumptions 4 and 6 imply that

$$\overset{\mathrm{G}_i\bullet}{\vec{\omega}}_{\mathrm{W}_i/\mathrm{G}_i} = 0$$

Thus, using Eq. (A8), the angular acceleration of $\mathrm{F_{W_i}}$ relative to $\mathrm{F_{G_i}}$ with respect to $\mathrm{F_B}$ is given by

$$\begin{aligned}\overset{\mathrm{B}\bullet}{\vec{\omega}}_{\mathrm{W}_i/\mathrm{G}_i} &= \overset{\mathrm{G}_i\bullet}{\vec{\omega}}_{\mathrm{W}_i/\mathrm{G}_i} + \vec{\omega}_{\mathrm{G}_i/\mathrm{B}} \times \vec{\omega}_{\mathrm{W}_i/\mathrm{G}_i} = \vec{\omega}_{\mathrm{G}_i/\mathrm{B}} \times \vec{\omega}_{\mathrm{W}_i/\mathrm{G}_i} \\ &= \vec{u}_i^{\times} \vec{\omega}_{\mathrm{W}_i/\mathrm{G}_i}\end{aligned} \tag{A21}$$

Because

$$\overset{\mathrm{B}\bullet}{\vec{r}}_{\mathrm{c}_i/\mathrm{c}} = 0$$

the derivative of the cross term in Eq. (A19) with respect to $\mathrm{F_B}$ is given by

$$\begin{aligned}\overset{\mathrm{B}\bullet}{\overbrace{\vec{r}^{\times 2}_{\mathrm{c}_i/\mathrm{c}}}} &= \vec{r}^{\times}_{\mathrm{c}_i/\mathrm{c}} \overset{\mathrm{B}\bullet}{\overbrace{\vec{r}^{\times}_{\mathrm{c}_i/\mathrm{c}}}} + \overset{\mathrm{B}\bullet}{\overbrace{\vec{r}^{\times}_{\mathrm{c}_i/\mathrm{c}}}} \vec{r}^{\times}_{\mathrm{c}_i/\mathrm{c}} = \vec{r}^{\times}_{\mathrm{c}_i/\mathrm{c}} (\overset{\mathrm{B}\bullet}{\vec{r}}_{\mathrm{c}_i/\mathrm{c}})^{\times} + (\overset{\mathrm{B}\bullet}{\vec{r}}_{\mathrm{c}_i/\mathrm{c}})^{\times} \vec{r}^{\times}_{\mathrm{c}_i/\mathrm{c}} \\ &= 0\end{aligned} \tag{A22}$$

Substituting Eqs. (A20–A22) into Eq. (A19) yields the derivative of Eq. (A9) with respect to $\mathrm{F_B}$; that is,

$$\begin{aligned}\overset{\mathrm{B}\bullet}{\vec{H}}_{\mathrm{W}_i/\mathrm{c/I}} &= (\vec{u}_i^{\times} \overrightarrow{J}_{\mathrm{W}_i/\mathrm{c}_i} - \overrightarrow{J}_{\mathrm{W}_i/\mathrm{c}_i} \vec{u}_i^{\times})(\vec{\omega}_{\mathrm{B/I}} + \vec{\omega}_{\mathrm{W}_i/\mathrm{G}_i} + \vec{u}_i) + \overrightarrow{J}_{\mathrm{W}_i/\mathrm{c}_i}(\vec{u}_i^{\times} \vec{\omega}_{\mathrm{W}_i/\mathrm{G}_i} + \overset{\mathrm{B}\bullet}{\vec{u}}_i) + \overrightarrow{J}_{\mathrm{W}_i/\mathrm{c}} \overset{\mathrm{B}\bullet}{\vec{\omega}}_{\mathrm{B/I}} \\ &= (\vec{u}_i^{\times} \overrightarrow{J}_{\mathrm{W}_i/\mathrm{c}_i} - \overrightarrow{J}_{\mathrm{W}_i/\mathrm{c}_i} \vec{u}_i^{\times})\vec{\omega}_{\mathrm{B/I}} + \vec{u}_i^{\times} \overrightarrow{J}_{\mathrm{W}_i/\mathrm{c}_i}(\vec{\omega}_{\mathrm{W}_i/\mathrm{G}_i} + \vec{u}_i) + \overrightarrow{J}_{\mathrm{W}_i/\mathrm{c}_i} \overset{\mathrm{B}\bullet}{\vec{u}}_i + \overrightarrow{J}_{\mathrm{W}_i/\mathrm{c}} \overset{\mathrm{B}\bullet}{\vec{\omega}}_{\mathrm{B/I}}\end{aligned} \tag{A23}$$

B. Resolving the Equations of Motion in $\mathrm{F_B}$

Resolving Poisson's equation [Eq. (1)] in $\mathrm{F_B}$ yields

$$\dot{\mathcal{R}}_{\mathrm{B/I}} = \frac{\mathrm{d}}{\mathrm{d}t}(\vec{R}_{\mathrm{B/I}}|_{\mathrm{B}}) = \overset{\mathrm{B}\bullet}{\vec{R}}_{\mathrm{B/I}}|_{\mathrm{B}} = \vec{R}_{\mathrm{B/I}}|_{\mathrm{B}} \vec{\omega}^{\times}_{\mathrm{B/I}}|_{\mathrm{B}} = \mathcal{R}_{\mathrm{B/I}} \omega^{\times}_{\mathrm{B}} \tag{B1}$$

where

$$\mathcal{R}_{\mathrm{B/I}} \triangleq \vec{R}_{\mathrm{B/I}}|_{\mathrm{B}} = \vec{R}_{\mathrm{B/I}}|_{\mathrm{I}}, \qquad \omega_{\mathrm{B}} \triangleq \vec{\omega}_{\mathrm{B/I}}|_{\mathrm{B}} \tag{B2}$$

Resolving Eq. (A1) in $\mathrm{F_B}$ yields

$$\vec{H}_{\mathrm{B/c/I}}|_{\mathrm{B}} = J_{\mathrm{B}} \omega_{\mathrm{B}} \tag{B3}$$

where

$$J_{\mathrm{B}} \triangleq \overrightarrow{J}_{\mathrm{B/c}}|_{\mathrm{B}} \tag{B4}$$

Furthermore, resolving Eq. (A18) in $\mathrm{F_B}$ yields

$$\overset{\mathrm{B}\bullet}{\vec{H}}_{\mathrm{B/c/I}}|_{\mathrm{B}} = \frac{\mathrm{d}}{\mathrm{d}t}(\vec{H}_{\mathrm{B/c/I}}|_{\mathrm{B}}) = J_{\mathrm{B}} \dot{\omega}_{\mathrm{B}} \tag{B5}$$

where

$$\dot{\omega}_{\mathrm{B}} = \overset{\mathrm{B}\bullet}{\vec{\omega}}_{\mathrm{B/I}}|_{\mathrm{B}} \tag{B6}$$

Using Fig. 3 and Assumptions 4, 5, and 6 to resolve the angular velocity of $\mathrm{F_{W_i}}$ relative to $\mathrm{F_{G_i}}$ in $\mathrm{F_{G_i}}$ yields

$$\vec{\omega}_{\mathrm{W}_i/\mathrm{G}_i}|_{\mathrm{G}_i} = \nu_i e_1 \tag{B7}$$

where $\nu_i > 0$ is the angular rate of W_i around $\hat{\imath}_{\mathrm{W}_i}$ relative to $\mathrm{F_{G_i}}$. Similarly, the gimbal angular velocity $\vec{u}_i$ defined by Eq. (A8) and the gimbal angular acceleration $\overset{\mathrm{G}_i\bullet}{\vec{u}}_i$ of $\mathrm{F_{G_i}}$ relative to $\mathrm{F_B}$ resolved in $\mathrm{F_{G_i}}$ are given by

$$\vec{u}_i|_{\mathrm{G}_i} = u_i e_2, \qquad \overset{\mathrm{G}_i\bullet}{\vec{u}}_i|_{\mathrm{G}_i} = \frac{\mathrm{d}}{\mathrm{d}t}(\vec{u}_i|_{\mathrm{G}_i}) = \dot{u}_i e_2 \tag{B8}$$

where u_i is the gimbal-rate request for CMG_i, and $\dot{u}_i$ is its derivative. Because u_i is the spin rate of g_i, the corresponding gimbal angle θ_i is defined such that

$$\dot{\theta}_i = u_i \tag{B9}$$

It thus follows from Eqs. (A8) and (B8) that

$$\vec{\omega}_{\mathrm{G}_i/\mathrm{B}}|_{\mathrm{G}_i} = \dot{\theta}_i e_2 \tag{B10}$$

Defining the gimbal angle vector $\theta \triangleq [\theta_1 \ \cdots \ \theta_n]^{\mathrm{T}}$ yields $\dot{\theta} = u$, where $u \triangleq [u_1 \ \cdots \ u_n]^{\mathrm{T}} \in \mathbb{R}^n$ is the control input. Furthermore, Fig. 3 and Assumptions 4 and 5 imply that the inertia matrix of W_i relative to c_i resolved in both $\mathrm{F}_{\mathrm{G}_i}$ and $\mathrm{F}_{\mathrm{W}_i}$ is given by

$$J_i \triangleq \overrightarrow{J}_{\mathrm{W}_i/\mathrm{c}_i}|_{\mathrm{G}_i} = \overrightarrow{J}_{\mathrm{W}_i/\mathrm{c}_i}|_{\mathrm{W}_i} = \begin{bmatrix} \alpha_i & 0 & 0 \\ 0 & \beta_i & 0 \\ 0 & 0 & \beta_i \end{bmatrix} \tag{B11}$$

where α_i is the moment of inertia of W_i around the spin axis $\hat{i}_{\mathrm{W}_i} = \hat{i}_{\mathrm{G}_i}$ and β_i is the moment of inertia around the remaining axes of $\mathrm{F}_{\mathrm{W}_i}$ and $\mathrm{F}_{\mathrm{G}_i}$.

Next, note that

$$\overset{\mathrm{B}\bullet}{\vec{u}}_i = \overset{\mathrm{G}_i\bullet}{\vec{u}}_i + \vec{\omega}_{\mathrm{G}_i/\mathrm{B}} \times \vec{u}_i = \overset{\mathrm{G}_i\bullet}{\vec{u}}_i \tag{B12}$$

Resolving Eqs. (B7), (B8), and (6) in F_{B} and using Eq. (B12) yield

$$\begin{aligned} &\vec{\omega}_{\mathrm{W}_i/\mathrm{G}_i}|_{\mathrm{B}} = \nu_i \mathcal{O}_i e_1, \qquad \vec{u}_i|_{\mathrm{B}} = \vec{\omega}_{\mathrm{G}_i/\mathrm{B}}|_{\mathrm{B}} = u_i \mathcal{O}_i e_2, \\ &\overset{\mathrm{B}\bullet}{\vec{u}}_i|_{\mathrm{B}} = \overset{\mathrm{G}_i\bullet}{\vec{u}}_i|_{\mathrm{B}} = \dot{u}_i \mathcal{O}_i e_2 \end{aligned} \tag{B13}$$

where

$$\overrightarrow{J}_{\mathrm{W}_i/\mathrm{c}_i}|_{\mathrm{B}} = \mathcal{O}_i \overrightarrow{J}_{\mathrm{W}_i/\mathrm{c}_i}|_{\mathrm{G}_i} \mathcal{O}_i^{\mathrm{T}} = \mathcal{O}_i J_i \mathcal{O}_i^{\mathrm{T}} \tag{B14}$$

and the orientation matrix $\mathcal{O}_i$ is defined by

$$\mathcal{O}_i \triangleq \overrightarrow{R}_{\mathrm{G}_i/\mathrm{B}}|_{\mathrm{G}_i} = \overrightarrow{R}_{\mathrm{G}_i/\mathrm{B}}|_{\mathrm{B}} \tag{B15}$$

where $\overrightarrow{R}_{\mathrm{G}_i/\mathrm{B}}$ is the rotation tensor that transforms F_{B} into $\mathrm{F}_{\mathrm{G}_i}$.

Resolving Eq. (A9) in F_{B} and using the fact that $\mathcal{O}_i^{\mathrm{T}} \mathcal{O}_i = \mathrm{I}_3$ yields

$$\begin{aligned} \vec{H}_{\mathrm{W}_i/\mathrm{c}/\mathrm{I}}|_{\mathrm{B}} &= \mathcal{O}_i J_i \mathcal{O}_i^{\mathrm{T}} (\nu_i \mathcal{O}_i e_1 + u_i \mathcal{O}_i e_2) + (\mathcal{O}_i J_i \mathcal{O}_i^{\mathrm{T}} - m_i r_i^{\times 2}) \omega_{\mathrm{B}} \\ &= \mathcal{O}_i (\alpha_i \nu_i e_1 + \beta_i u_i e_2) + J_{i,\mathrm{c}} \omega_{\mathrm{B}} \end{aligned} \tag{B16}$$

Furthermore, define

$$J_{i,\mathrm{c}} \triangleq \overrightarrow{J}_{\mathrm{W}_i/\mathrm{c}}|_{\mathrm{B}} = \mathcal{O}_i J_i \mathcal{O}_i^{\mathrm{T}} - m_i r_i^{\times 2}, \qquad r_i \triangleq \vec{r}_{\mathrm{c}_i/\mathrm{c}}|_{\mathrm{B}} \tag{B17}$$

Using Eq. (B16) to resolve the sum in Eq. (A11) in F_{B} yields

$$\begin{aligned} \sum_{i=1}^{n} \vec{H}_{\mathrm{W}_i/\mathrm{c}/\mathrm{I}}|_{\mathrm{B}} &= \sum_{i=1}^{n} [\mathcal{O}_i (\alpha_i \nu_i e_1 + \beta_i u_i e_2) + J_{i,\mathrm{c}} \omega_{\mathrm{B}}] \\ &= \sum_{i=1}^{n} (\alpha_i \nu_i \mathcal{O}_i e_1 + J_{i,\mathrm{c}} \omega_{\mathrm{B}}) - \mathrm{B}_1 u \end{aligned} \tag{B18}$$

where the ith column of $\mathrm{B}_1 \in \mathbb{R}^{3\times n}$ is given by

$$B_{1i} = -\beta_i \mathcal{O}_i e_2 \in \mathbb{R}^3 \tag{B19}$$

Using Eqs. (1) and (A8), it follows that

$$\dot{\mathcal{O}}_i = \overset{\mathrm{G}_i\bullet}{\overrightarrow{R}}_{\mathrm{G}_i/\mathrm{B}}|_{\mathrm{G}_i} = \overrightarrow{R}_{\mathrm{G}_i/\mathrm{B}} \vec{u}_i^{\times}|_{\mathrm{G}_i} = \mathcal{O}_i u_i e_2^{\times} \tag{B20}$$

Therefore,

$$\dot{B}_{1i} = -\beta_i \dot{\mathcal{O}}_i e_2 = -\beta_i \mathcal{O}_i u_i e_2^{\times} e_2 = 0 \tag{B21}$$

which implies that B_1 in Eq. (B18) is constant.

Resolving Eq. (A23) in F_{B} yields the derivative of Eq. (B16), which is given by

$$\begin{aligned} \frac{\mathrm{d}}{\mathrm{d}t}(\vec{H}_{\mathrm{W}_i/\mathrm{c}/\mathrm{I}}|_{\mathrm{B}}) &= \overset{\mathrm{B}\bullet}{\vec{H}}_{\mathrm{W}_i/\mathrm{c}/\mathrm{I}}|_{\mathrm{B}} = u_i \mathcal{O}_i (e_2^{\times} J_i - J_i e_2^{\times}) \mathcal{O}_i^{\mathrm{T}} \omega_{\mathrm{B}} \\ &\quad + \mathcal{O}_i (u_i e_2)^{\times} \mathcal{O}_i^{\mathrm{T}} \mathcal{O}_i J_i (u_i e_2 + \nu_i e_1) + \dot{u}_i \mathcal{O}_i J_i e_2 + J_{i,\mathrm{c}} \dot{\omega}_{\mathrm{B}} \\ &= u_i \mathcal{O}_i (e_2^{\times} J_i - J_i e_2^{\times}) \mathcal{O}_i^{\mathrm{T}} \omega_{\mathrm{B}} + u_i \mathcal{O}_i (e_2^{\times} \beta_i u_i e_2 + e_2^{\times} \alpha_i \nu_i e_1) \\ &\quad + \dot{u}_i \mathcal{O}_i \beta_i e_2 + J_{i,\mathrm{c}} \dot{\omega}_{\mathrm{B}} \\ &= [\mathcal{O}_i (e_2^{\times} J_i - J_i e_2^{\times}) \mathcal{O}_i^{\mathrm{T}} \omega_{\mathrm{B}} - \alpha_i \nu_i \mathcal{O}_i e_3] u_i + \beta_i \dot{u}_i \mathcal{O}_i e_2 + J_{i,\mathrm{c}} \dot{\omega}_{\mathrm{B}} \end{aligned} \tag{B22}$$

Using Eqs. (B19) and (B22) to resolve the sum in Eq. (A17) in F_{B} yields

$$\begin{aligned} \sum_{i=1}^{n} \overset{\mathrm{B}\bullet}{\vec{H}}_{\mathrm{W}_i/\mathrm{c}/\mathrm{I}}|_{\mathrm{B}} &= \sum_{i=1}^{n} (J_{i,\mathrm{c}} \dot{\omega}_{\mathrm{B}} - B_{1i} \dot{u}_i + B_{2i} u_i) \\ &= \left(\sum_{i=1}^{n} J_{i,\mathrm{c}} \dot{\omega}_{\mathrm{B}} \right) - B_1 \dot{u} + B_2 u \end{aligned} \tag{B23}$$

where $\dot{u} = [\dot{u}_1 \ \cdots \ \dot{u}_n]^{\mathrm{T}}$, and the ith column of $B_2 \in \mathbb{R}^{3\times n}$ is given by

$$B_{2i} = \mathcal{O}_i (e_2^{\times} J_i - J_i e_2^{\times}) \mathcal{O}_i^{\mathrm{T}} \omega_{\mathrm{B}} - \alpha_i \nu_i \mathcal{O}_i e_3 \in \mathbb{R}^3 \tag{B24}$$

Using Eqs. (B3) and (B18) to resolve Eq. (A11) in F_{B} yields

$$H_{\mathrm{SC}} \triangleq \vec{H}_{\mathrm{SC}/\mathrm{c}/\mathrm{I}}|_{\mathrm{B}} = J \omega_{\mathrm{B}} + \sum_{i=1}^{n} \alpha_i \nu_i \mathcal{O}_i e_1 - \mathrm{B}_1 u \tag{B25}$$

where, using Eq. (A13),

$$J \triangleq \overrightarrow{J}_{\mathrm{SC}/\mathrm{c}}|_{\mathrm{B}} = J_{\mathrm{B}} + \sum_{i=1}^{n} J_{i,\mathrm{c}} \tag{B26}$$

Using Eqs. (B5) and (B23) to resolve Eq. (A17) in F_{B} yields

$$\dot{H}_{\mathrm{SC}} = \frac{\mathrm{d}}{\mathrm{d}t}(\vec{H}_{\mathrm{SC}/\mathrm{c}/\mathrm{I}}|_{\mathrm{B}}) = \overset{\mathrm{B}\bullet}{\vec{H}}_{\mathrm{SC}/\mathrm{c}/\mathrm{I}}|_{\mathrm{B}} = J \dot{\omega}_{\mathrm{B}} - B_1 \dot{u} + B_2 u \tag{B27}$$

Resolving Eq. (A16) in F_{B} using Eqs. (B25) and (B27) yields

$$J \dot{\omega}_{\mathrm{B}} - B_1 \dot{u} + B_2 u = -\omega_{\mathrm{B}} \times \left(J \omega_{\mathrm{B}} + \sum_{i=1}^{n} \alpha_i \nu_i \mathcal{O}_i e_1 - B_1 u \right) + \tau_{\mathrm{dist}} \tag{B28}$$

where the torque applied to the spacecraft by the disturbances is given by

$$\tau_{\mathrm{dist}} \triangleq \vec{M}_{\mathrm{dist}}|_{\mathrm{B}} \tag{B29}$$

Rearranging Eq. (B28) yields the dynamics for a spacecraft actuated by n angular-velocity-requested single-gimbal constant-angular-rate CMGs subject to external torque disturbances; that is,

$$J\dot{\omega}_{\mathrm{B}} + \omega_{\mathrm{B}} \times \left(J\omega_{\mathrm{B}} + \sum_{i=1}^{n} \alpha_i \nu_i \mathcal{O}_i e_1 \right) = \tau_{\mathrm{CMG}} + \tau_{\mathrm{dist}} \tag{B30}$$

where the torque τ_{CMG} applied to the spacecraft by the CMGs is given by

$$\tau_{\mathrm{CMG}} \triangleq B_{\mathrm{CMG}} u + B_1 \dot{u} \tag{B31}$$

where

$$B_{\mathrm{CMG}} \triangleq \omega_{\mathrm{B}}^{\times} B_1 - B_2 \in \mathbb{R}^{3\times n} \tag{B32}$$

If the wheel angular rate ν_i is much larger than the maximum component of the bus angular velocity (that is, $|\nu_i| \gg |\max\{\omega_1, \omega_2, \omega_3\}|$), then it follows from Eqs. (B19), (B24), and (B32) that

$$B_{\mathrm{CMG},i} \approx \alpha_i \nu_i \mathcal{O}_i e_3 \tag{B33}$$

which is not necessarily constant due to $\mathcal{O}_i$. The simplified matrix [Eq. (B33)] is the Jacobian used in Refs. [5,13] to formulate torque-steering laws and analyze gimbal singularities.

C. Time Dependence of J and B_{CMG}

The rotation rate of the gimbals due to the requested gimbal rates u changes the gimbal configuration, and thus the inertia of the spacecraft. Therefore, J may be time varying. Using Eqs. (B17) and (B26), the spacecraft inertia is expressed as

$$J = J_{\mathrm{B}} + \sum_{i=1}^{n} (\mathcal{O}_i J_i \mathcal{O}_i^{\mathrm{T}} - m_i r_i^{\times 2}) \tag{C1}$$

where Assumption 1 implies that J_{B} and J_i are constant. Therefore,

$$\dot{J} = \sum_{i=1}^{n} \dot{\mathcal{O}}_i J_i \mathcal{O}_i^{\mathrm{T}} + \mathcal{O}_i J_i \dot{\mathcal{O}}_i^{\mathrm{T}} = \sum_{i=1}^{n} u_i \mathcal{O}_i (e_2^{\times} J_i - J_i e_2^{\times}) \mathcal{O}_i^{\mathrm{T}} \tag{C2}$$

The control input matrix B_{CMG} defined by Eq. (B32) has a similar dependence on u. Using Eqs. (B21) and (B30) to rewrite the derivative of Eq. (B32) yields

$$\dot{B}_{\mathrm{CMG}} = \dot{\omega}_{\mathrm{B}}^{\times} B_1 - \dot{B}_2 \tag{C3}$$

Solving Eq. (B30) for $\dot{\omega}_{\mathrm{B}}$ yields

$$\dot{\omega}_{\mathrm{B}} = J^{-1} \left[-\omega_{\mathrm{B}}^{\times} \left(J\omega_{\mathrm{B}} + \sum_{i=1}^{n} \alpha_i \nu_i \mathcal{O}_i e_1 \right) + B_{\mathrm{CMG}} u + B_1 \dot{u} + \tau_{\mathrm{dist}} \right] \tag{C4}$$

Note that the term $\dot{\omega}_{\mathrm{B}}^{\times} B_1$ in Eq. (C3) depends on u and τ_{dist} due to Eq. (C4). The derivative of the ith column B_{2i} of B_2, defined by Eq. (B24), is given by

$$\begin{aligned} \dot{B}_{2i} = {} & u_i \mathcal{O}_i [e_2^{\times} (e_2^{\times} J_i - J_i e_2^{\times}) - (e_2^{\times} J_i - J_i e_2^{\times}) e_2^{\times}] \mathcal{O}_i^{\mathrm{T}} \omega_{\mathrm{B}} \\ & + \mathcal{O}_i (e_2^{\times} J_i - J_i e_2^{\times}) \mathcal{O}_i^{\mathrm{T}} \dot{\omega}_{\mathrm{B}} - \alpha_i \nu_i \mathcal{O}_i u_i e_1 \end{aligned} \tag{C5}$$

Therefore, the term $\dot{B}_2$ in Eq. (C3) depends on u directly as well as indirectly through its dependence on $\dot{\omega}_{\mathrm{B}}$ given by Eq. (C4). Furthermore, Eq. (C5) also depends on τ_{dist} due to Eq. (C4). Hence, both terms in Eq. (C3) depend on the control input u and the external torque τ_{dist}. Consequently, B_{CMG} may be time varying.

References

[1] Carpenter, M. D., and Peck, M. A., "Reducing Base Reactions with Gyroscopic Actuation of Space-Robotic Systems," *IEEE Transactions on Robotics*, Vol. 25, No. 6, 2009, pp. 1262–1270. doi:10.1109/TRO.2009.2032953

[2] Schaub, H., and Junkins, J. L., *Analytical Mechanics of Space Systems*, 2nd ed., AIAA, Reston, VA, 2003, p. 264. doi:10.2514/4.867231

[3] Wie, B., *Space Vehicle Dynamics and Control*, 2nd ed., AIAA, Reston, VA, 2008, p. 461. doi:10.2514/4.860119

[4] Leve, F., Hamilton, B., and Peck, M., *Spacecraft Momentum Control Systems*, Springer, New York, 2015, p. 157. doi:10.1007/978-3-319-22563-0

[5] Wie, B., "Singularity Analysis and Visualization for Single-Gimbal Control Moment Gyro Systems," *Journal of Guidance, Control, and Dynamics*, Vol. 27, No. 2, 2004, pp. 271–282. doi:10.2514/1.9167

[6] Paradiso, J. A., "Global Steering of Single Gimbaled Control Moment Gyroscopes Using a Directed Search," *Journal of Guidance, Control, and Dynamics*, Vol. 15, No. 5, 1992, pp. 1236–1244. doi:10.2514/3.20974

[7] Kurokawa, H., "A Geometric Study of Single Gimbal Control Moment Gyros," *Report of Mechanical Engineering Laboratory*, Vol. 175, Jan. 1998, pp. 135–138.

[8] Bedrossian, N. S., Paradiso, J., Bergmann, E. V., and Rowell, D., "Redundant Single Gimbal Control Moment Gyroscope Singularity Analysis," *Journal of Guidance, Control, and Dynamics*, Vol. 13, No. 6, 1990, pp. 1096–1101. doi:10.2514/3.20584

[9] Schaub, H., Vadali, S., and Junkins, J., "Feedback Control Law for Variable Speed Control Moment Gyros," *Journal of the Astronautical Sciences*, Vol. 46, No. 3, 1998, pp. 307–328.

[10] Yoon, H., and Tsiotras, P., "Singularity Analysis of Variable-Speed Control Moment Gyros," *Journal of Guidance, Control, and Dynamics*, Vol. 27, No. 3, 2004, pp. 374–386. doi:10.2514/1.2946

[11] Viswanathan, S. P., Sanyal, A. K., Leve, F., and McClamroch, N. H., "Dynamics and Control of Spacecraft with a Generalized Model of Variable Speed Control Moment Gyroscopes," *Journal of Dynamic Systems, Measurement and Control*, Vol. 137, No. 7, 2007, Paper 071003.

[12] Prabhakaran, V. S., and Sanyal, A., "Adaptive Singularity-Free Control Moment Gyroscopes," *Journal of Guidance, Control, and Dynamics*, Vol. 41, No. 11, 2018, pp. 2416–2424. doi:10.2514/1.G003545

[13] Leve, F. A., "Evaluation of Steering Algorithm Optimality for Single-Gimbal Control Moment Gyroscopes," *IEEE Transactions on Control Systems Technology*, Vol. 22, No. 3, 2014, pp. 1130–1134. doi:10.1109/TCST.2013.2259829

[14] Takada, K., Kojima, H., and Matsuda, N., "Control Moment Gyro Singularity-Avoidance Steering Control Based on Singular-Surface Cost Function," *Journal of Guidance, Control, and Dynamics*, Vol. 33, No. 5, 2010, pp. 1442–1450. doi:10.2514/1.48381

[15] Wang, L., Guo, Y., Wu, L., and Chen, Q., "Improved Optimal Steering Law for SGCMG and Adaptive Attitude Control of Flexible Spacecraft," *Journal of Systems Engineering and Electronics*, Vol. 26, No. 6, 2015, pp. 1268–1276. doi:10.1109/JSEE.2015.00139

[16] Elliott, D. S., Peck, M. A., and Nesnas, I., "Novel Method for Control Moment Gyroscope Singularity Avoidance Using Constraints," *AIAA Guidance, Navigation, and Control Conference, AIAA SciTech Forum*, AIAA Paper 2018-1327, 2018. doi:10.2514/6.2018-1327

[17] Geng, Y., Hou, Z., and Huang, S., "Global Singularity Avoidance Steering Law for Single-Gimbal Control Moment Gyroscopes," *Journal of Guidance, Control, and Dynamics*, Vol. 40, No. 11, 2017, pp. 3027–3036. doi:10.2514/1.G002331

[18] Geng, Y., Hou, Z., Guo, J., and Huang, S., "Rapid Singularity-Escape Steering Strategy for Single-Gimbal Control Moment Gyroscopes," *Journal of Guidance, Control, and Dynamics*, Vol. 40, No. 12, 2017, pp. 3199–3210. doi:10.2514/1.G002686

[19] Valk, L., Berry, A., and Vallery, H., "Directional Singularity Escape and Avoidance for Single-Gimbal Control Moment Gyroscopes," *Journal of Guidance, Control, and Dynamics*, Vol. 41, No. 5, 2018, pp. 1095–1107. doi:10.2514/1.G003132

[20] Jones, L. L., Zeledon, R. A., and Peck, M. A., "Generalized Framework for Linearly Constrained Control Moment Gyro Steering," *Journal of*

Guidance, Control, and Dynamics, Vol. 35, No. 4, 2012, pp. 1094–1103.
doi:10.2514/1.56207

[21] Gersh, J., and Peck, M., "Violet: A High-Agility Nanosatellite for Demonstrating Small Control-Moment Gyroscope Prototypes and Steering Laws," *Guidance, Navigation, and Control Conference*, AIAA Paper 2009-5900, 2009.
doi:10.2514/6.2009-5900

[22] Zhang, J., Ma, K., Meng, G., and Tian, S., "Spacecraft Maneuvers via Singularity-Avoidance of Control Moment Gyros Based on Dual-Mode Model Predictive Control," *IEEE Transactions on Aerospace and Electronic Systems*, Vol. 51, No. 4, 2015, pp. 2546–2559.
doi:10.1109/TAES.2015.130715

[23] Takada, K., and Kojima, H., "Receding Horizon Control on Steering of Control Moment Gyro for Fast Attitude Maneuver," *Transactions of the Japan Society for Aeronautical and Space Sciences*, Vol. 52, No. 175, 2009, pp. 1–10.
doi:10.2322/tjsass.52.1

[24] Guo, Y., Cui, H., Ma, G., and Li, C., "Singular Direction Escape Steering Law for Control Moment Gyros," *Journal of Aerospace Engineering*, Vol. 30, No. 5, 2017, pp. 648–656.
doi:10.2514/2.4610

[25] MacKunis, W., Dupree, K., FitzCoy, N., and Dixon, W. E., "Adaptive Satellite Attitude Control in the Presence of Inertia and CMG Gimbal Friction Uncertainties," *Journal of Astronautical Sciences*, Vol. 56, No. 1, 2008, pp. 121–134.
doi:10.1007/BF03256544

[26] Wang, L., Zhong, C., Guo, Y., Wu, Y., and Guo, J., "Robust Adaptive Attitude Control for Flexible Spacecraft in the Presence of SGCMG Friction Nonlinearity," *International Journal of Robust and Nonlinear Control*, Vol. 28, No. 9, 2018, pp. 3324–3341.
doi:10.1002/rnc.v28.9

[27] MacKunis, W., Leve, F., Patre, P., Fitz-Coy, N., and Dixon, W., "Adaptive Neural Network-Based Satellite Attitude Control in the Presence of CMG Uncertainty," *Aerospace Science and Technology*, Vol. 54, July 2016, pp. 218–228.
doi:10.1016/j.ast.2016.04.022

[28] Cui, P., and Liu, F., "Attitude-Tracking Control with Path Planning for Agile Satellite Using Double-Gimbal Control Moment Gyros," *Mathematical Problems in Engineering*, Vol. 2012, 2012, pp. 1–19.
doi:10.1155/2012/342043

[29] Yoon, H., and Tsiotras, P., "Spacecraft Adaptive Attitude and Power Tracking with Variable Speed Control Moment Gyroscopes," *Journal of Guidance, Control, and Dynamics*, Vol. 25, No. 6, 2002, pp. 1081–1090.
doi:10.2514/2.4987

[30] Yoon, H., and Agrawal, B. N., "Adaptive Control of Uncertain Hamiltonian Multi-Input Multi-Output Systems with Application to Spacecraft Control," *Proceedings of the American Control Conference*, IEEE Publ., Piscataway, NJ, 2008, pp. 2969–2974.
doi:10.1109/ACC.2008.4586947

[31] Sun, Z., and Ding, S., "SGCMG Non-Singularity Steering Based on Adaptive Gauss Pseudospectral Method," *International Conference on Informative and Cybernetics for Computational Social Systems*, IEEE Publ., Piscataway, NJ, 2014, pp. 96–101.
doi:10.1109/ICCSS.2014.6961823

[32] Ozawa, R., and Takahashi, M., "Agile Attitude Control and Singularity Avoidance/Escape by the SDRE Method Using a Biased State-Dependent Weighting Matrix," *Applied Sciences*, Vol. 8, No. 1, 2018, Paper 140.
doi:10.3390/app8010140

[33] Zhang, F., Jin, L., and Xu, S., "Fault Tolerant Attitude Control for Spacecraft with SGCMGs Under Actuator Partial Failure and Actuator Saturation," *Acta Astronautica*, Vol. 132, March 2017, pp. 303–311.
doi:10.1016/j.actaastro.2016.12.033

[34] Santillo, M. A., and Bernstein, D. S., "Adaptive Control Based on Retrospective Cost Optimization," *Journal of Guidance, Control, and Dynamics*, Vol. 33, No. 2, 2010, pp. 289–304.
doi:10.2514/1.46741

[35] Hoagg, J. B., and Bernstein, D., "Retrospective Cost Model Reference Adaptive Control for Nonminimum-Phase Systems," *Journal of Guidance, Control, and Dynamics*, Vol. 35, No. 6, 2012, pp. 1767–1786.
doi:10.2514/1.57001

[36] Rahman, Y., Xie, A., and Bernstein, D. S., "Retrospective Cost Adaptive Control: Pole Placement, Frequency Response, and Connections with LQG Control," *IEEE Control Systems*, Vol. 37, No. 5, 2017, pp. 28–69.
doi:10.1109/MCS.2017.2718825

[37] Chaturvedi, N., Sanyal, A. K., and McClamroch, N. H., "Rigid Body Attitude Control," *IEEE Control Systems Magazine*, Vol. 31, No. 3, 2011, pp. 30–51.
doi:10.1109/MCS.2011.940459

[38] Sanyal, A., Fosbury, A., Chaturvedi, N., and Bernstein, D. S., "Inertia-Free Spacecraft Attitude Tracking with Disturbance Rejection and Almost Global Stabilization," *Journal of Guidance, Control, and Dynamics*, Vol. 32, No. 4, 2009, pp. 1167–1178.
doi:10.2514/1.41565

[39] Agarwal, K., Weiss, A., Kolmanovsky, I., and Bernstein, D. S., "Inertia-Free Spacecraft Attitude Control with Control-Moment-Gyro Actuation," *AIAA Guidance, Navigation, and Control Conference*, AIAA Paper 2012-5003, 2012.
doi:10.2514/6.2012-5003

[40] Camblor, M., Cruz, G., Esteban, S., Leve, F. A., and Bernstein, D. S., "Retrospective Cost Adaptive Spacecraft Attitude Control Using Control Moment Gyros," *Proceedings of the American Control Conference*, IEEE Publ., Piscataway, NJ, 2014, pp. 2492–2497.
doi:10.1109/ACC.2014.6859136

[41] Cruz, G., and Bernstein, D. S., "Adaptive Spacecraft Attitude Control with Reaction Wheel Actuation," *Proceedings of the American Control Conference*, IEEE Publ., Piscataway, NJ, 2013, pp. 4832–4837.
doi:10.1109/ACC.2013.6580586

[42] Cruz, G., and Bernstein, D. S., "Retrospective Cost Adaptive Control of Spacecraft Attitude Using Magnetic Actuators," *AIAA Guidance, Navigation, and Control Conference*, AIAA Paper 2013-4563, 2013.
doi:10.2514/6.2013-4563

[43] Zhao, Z., Cruz, G., Lee, T., and Bernstein, D. S., "Adaptive Attitude Control of a Dual-Rigid-Body Spacecraft with Unmodeled Non-minimum-Phase Dynamics," *2018 Annual American Control Conference (ACC)*, IEEE Publ., Piscataway, NJ, 2018, pp. 2503–2508.
doi:10.23919/ACC.2018.8431163

[44] Vadali, S., "Feedback Control and Steering Laws for Spacecraft Using Single Gimbal Control Moment Gyros," *Guidance, Navigation and Control Conference*, AIAA Paper 1988-3475, 1988.
doi:10.2514/6.1989-3475

[45] Asghar, S., "Exact Steering in Control Moment Gyroscope Systems," Ph.D. Thesis, Univ. of Surrey, Guildford, England, U.K., 2008.

[46] Bernstein, D. S., *Scalar, Vector, and Matrix Mathematics: Theory, Facts, and Formulas*, Princeton Univ. Press, Princeton, NJ, 2018, p. 388.

[47] Morozov, A. V., Hoagg, J. B., and Bernstein, D. S., "Retrospective Cost Adaptive Control of a Planar Multilink Arm with Nonminimum-Phase Zeros," *Proceedings of the IEEE Conference on Decision and Control*, IEEE Publ., Piscataway, NJ, 2010, pp. 3706–3711.
doi:10.1109/CDC.2010.5718121

[48] Weiss, A., Kolmanovsky, I., Bernstein, D. S., and Sanyal, A., "Inertia-Free Spacecraft Attitude Control Using Reaction Wheels," *Journal of Guidance, Control, and Dynamics*, Vol. 36, No. 5, 2013, pp. 1425–1439.
doi:10.2514/1.58363

[49] Hu, Q., Li, B., and Zhang, A., "Robust Finite-Time Control Allocation in Spacecraft Attitude Stabilization Under Actuator Misalignment," *Nonlinear Dynamics*, Vol. 73, Nos. 1–2, 2013, pp. 53–71.
doi:10.1007/s11071-013-0766-2

[50] Mercker, T. H., and Akella, M. R., "Adaptive Estimation and Control Algorithms for Certain Independent Control Axis Misalignments," *Journal of Guidance, Control, and Dynamics*, Vol. 37, No. 1, 2014, pp. 72–85.
doi:10.2514/1.61735